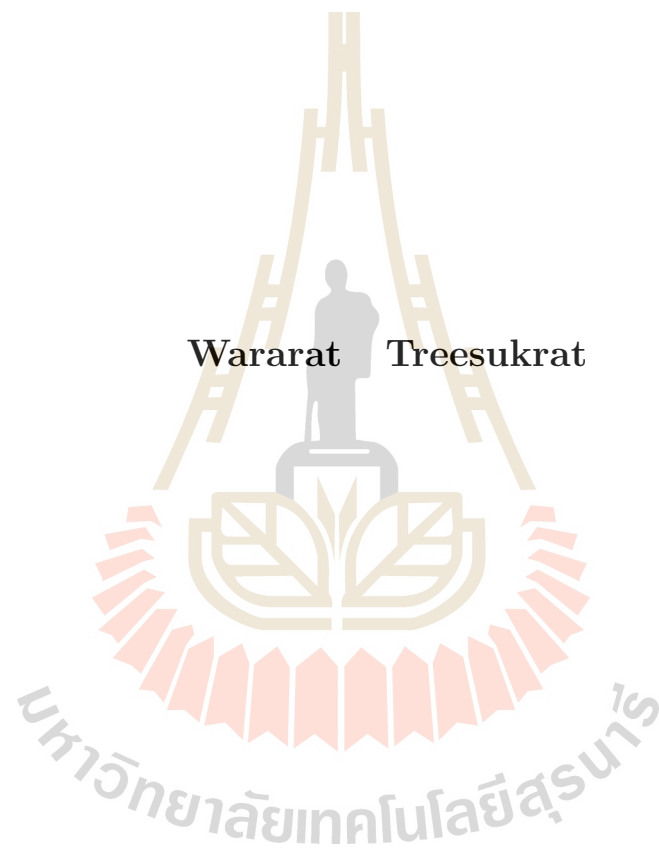


NEUTRINO PROPERTIES IN MODEL WITH GAUGED LEPTON FLAVOR



A Thesis Submitted in Partial Fulfillment of the Requirements for the
Degree of Master of Science in Physics
Suranaree University of Technology
Academic Year 2018

สมบัตินิวทรีโนในโมเดลของเกจเลปตอนเฟลเวอร์



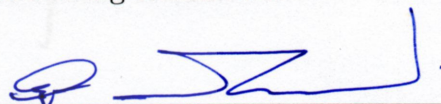
นางสาววรารัตน์ ตรีสุขรัตน์

วิทยานิพนธ์นี้เป็นส่วนหนึ่งของการศึกษาตามหลักสูตรปริญญาวิทยาศาสตรมหาบัณฑิต
สาขาวิชาฟิสิกส์
มหาวิทยาลัยเทคโนโลยีสุรนารี
ปีการศึกษา 2561

NEUTRINO PROPERTIES IN MODEL WITH GAUGED LEPTON FLAVOR

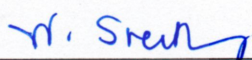
Suranaree University of Technology has approved this thesis submitted in partial fulfillment of the requirements for the Degree of Master.

Thesis Examining Committee



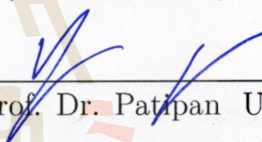
(Asst. Prof. Dr. Ayut Limphirat)

Chairperson



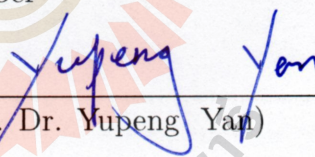
(Dr. Warintorn Sreethawong)

Member (Thesis Advisor)



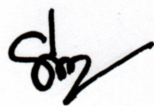
(Asst. Prof. Dr. Patipan Uttayarat)

Member



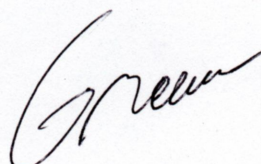
(Prof. Dr. Yupeng Yan)

Member



(Prof. Dr. Santi Maensiri)

Vice Rector for Academic Affairs
and Internationalization



(Assoc. Prof. Dr. Worawat Meevasana)

Dean of Institute of Science

วรารัตน์ ศรีสุวรรณ์ : สมบัตินิวตริโนในโมเดลของเกจเลปตอนเฟลเวอร์ (NEUTRINO PROPERTIES IN MODEL WITH GAUGED LEPTON FLAVOR). อาจารย์ที่ปรึกษา : อาจารย์ ดร. วรินทร์ ศรีทะวงศ์, 69 หน้า.

การมีอยู่ของนิวตริโนที่มีมวล เป็นหลักฐานหนึ่งของการมีอยู่ของโมเดลที่นอกเหนือโมเดลมาตรฐาน โมเดลของเกจเลปตอนเฟลเวอร์เป็นโมเดลหนึ่งที่ถูกนำเสนอเพื่อรองรับการมีอยู่ของนิวตริโนที่มีมวล ในโมเดลนี้ เฟอร์มิออนสามชนิดถูกเสนอขึ้นมาหักล้างความผิดปกติของเกจ นั่นคือ \mathcal{E}_R , \mathcal{E}_L และ N_R โดยเฟอร์มิออนทั้งสามชนิดนี้จะนำไปสู่กลไกไมกระดกเพื่อที่จะสร้างมวลของนิวตริโน ค่าคงตัวยูคาวา จะถูกเสนอให้เป็นสนามสเกลาร์ หรือ สนามของเฟลวอน นั่นคือ Y_E และ Y_N ทั้งสองสนามเฟลวอนนี้สามารถดำเนินการแปลงภายใต้ $SU(3)_L \times SU(3)_E$

เนื่องจากการที่เงื่อนไขจากข้อมูลการทดลอง ไม่สามารถคำนวณหาขอบล่างของมวลของนิวตริโนที่เบาที่สุดได้ เงื่อนไขของพาร์เทียวเวฟยูนิทาลิตี จึงถูกนำมาพิจารณาเพิ่มเติมเพื่อหาขอบล่างนั้นออกมา จากนั้นเพื่อที่จะได้สเปกตรัมของนิวตริโนที่เป็นไปได้ เราจะใช้เทคนิคนี้ลงไปในการคำนวณแอมพลิจูดในกระบวนการต่าง ๆ ขอบเขตมวลของเกจโบซอนจะถูกคำนวณหาและมันสัมพันธ์กับมวลของนิวตริโนอย่างแปรผกผัน สุดท้ายนี้ เงื่อนไขของพาร์เทียวเวฟยูนิทาลิตีจะสามารถคำนวณหาขอบล่างของมวลที่เบาที่สุดของนิวตริโนได้จากกระบวนการ $F^i \bar{F}^i \rightarrow A_L^{L,a} A_L^{L,a}$ และ $F^i \bar{F}^j \rightarrow A_L^{L,a} A_L^{L,b}$ แต่ไม่สามารถคำนวณหาเงื่อนไขขอบเขตของตัวแปรของมิกซ์ซึ่งนิวตริโนได้

สาขาวิชาฟิสิกส์
ปีการศึกษา 2561

ลายมือชื่อนักศึกษา วรารัตน์ ศรีสุวรรณ์

ลายมือชื่ออาจารย์ที่ปรึกษา ท. วรินทร์

ลายมือชื่ออาจารย์ที่ปรึกษาร่วม [ลายมือ]

WARARAT TREESUKRAT : NEUTRINO PROPERTIES IN MODEL
WITH GAUGED LEPTON FLAVOR. THESIS ADVISOR :
WARINTORN SREETHAWONG, Ph.D. 69 PP.

NEUTRINO/GAUGED LEPTON MODEL/PARTIAL WAVE UNITARY
CONSTRAINT

Massive neutrino is one of beyond the Standard model evidences. The model with gauged lepton flavor is one of the models which can address massive neutrino. In this model, three new species of fermion were introduced to cancel gauge anomalies, i.e. \mathcal{E}_R , \mathcal{E}_L and \mathcal{N}_R . These new fermions lead to a see-saw mechanism for neutrino mass generation. Yukawa couplings were promoted to scalar fields (flavon fields), i.e. \mathcal{Y}_E and \mathcal{Y}_N . These flavon fields transform under $SU(3)_\ell \times SU(3)_E$.

Since only constraints from the current experimental data cannot determine the lower bound on the lightest neutrino mass, partial wave unitary constraint (PWUC) was added to rule it out. To obtain the viable neutrino spectrum, the PWUC was applied on 2-2 scattering processes. Masses of gauge bosons were bounded and they are inversely proportional to neutrino masses. Finally, the lower bound on the lightest neutrino mass can be determined by the PWUC from processes $F^i \bar{F}^j \rightarrow A_L^{l,a} A_L^{l,b}$ and $F^i \bar{F}^i \rightarrow A_L^{l,a} A_L^{l,a}$. Unfortunately, the PWUC cannot give a meaningful constraint on mixing parameters.

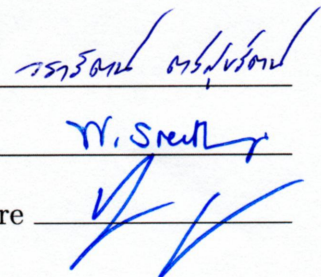
School of Physics

Academic Year 2018

Student's Signature

Advisor's Signature

Co-advisor's Signature



ACKNOWLEDGEMENTS

I would like to express my appreciation to all supports and inspirations in my physics student life. First of my appreciation goes for my supervisors Dr. Warintorn Sreethawong and Asst. Prof. Patipan Uttayarat from Srinakharinwirot University, Thailand. They give me all best supports, advises and inspirations. Especially, Asst. Prof. Dr. Patipan Uttayarat who calmly teaches me how to deal with unexpected results. Without doubt, It is a wonderful research experiences.

Next, I would like to express my gratitude for Prof. Yupeng Yan and Asst. Prof. Dr. Ayut Limphirat who always support and give me the best opportunities in many particle physics conferences or group discussions. Next, I would like to thank all of my physics lecturers. They taught me not only academic knowledge but also how to think as scientist. I also would like to thank my friends in the high energy and particle physics group at SUT and the theoretical high-energy physics and astrophysics group at SWU, who fulfill my questions and answers in many physics classes.

Last but not least, I would like to thank my family, who even does not know what my research is or what am I study but they always support me in everything about my study. Their all unconditional love and care motivated me to do all my best in this thesis. Without doubt again, I would like to give my sincere gratitude for them.

Wararat Treesukrat

CONTENTS

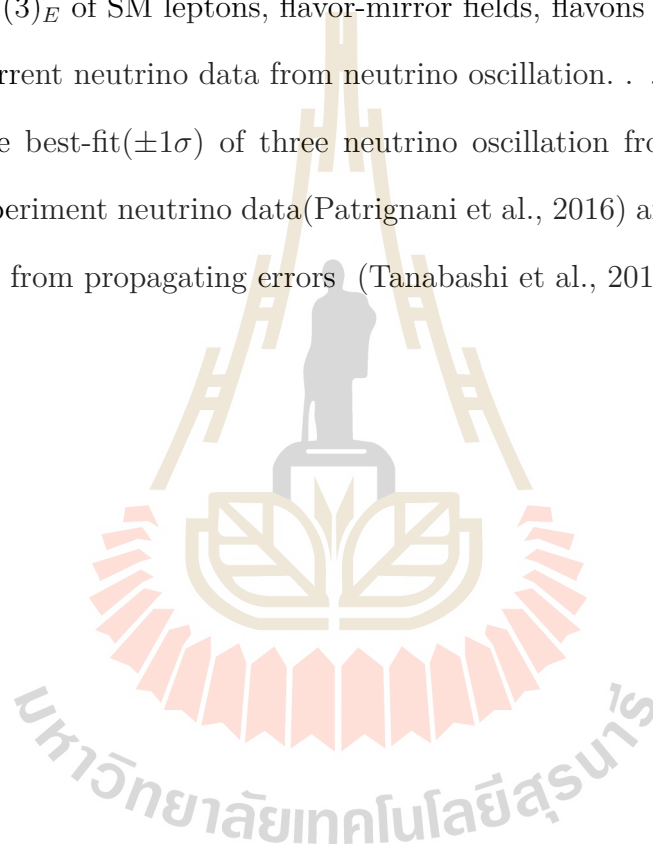
	Page
ABSTRACT IN THAI	I
ABSTRACT IN ENGLISH	II
ACKNOWLEDGEMENTS	III
CONTENTS	V
LIST OF TABLES	VII
LIST OF FIGURES	VIII
LIST OF ABBREVIATIONS	IX
CHAPTER	
I INTRODUCTION	1
II GAUGED LEPTON FLAVOR MODEL	4
1. Interactions	5
2. Flavor gauge lepton mass	6
III SCATTERING AMPLITUDES	13
1. $F^i \bar{F}^i \rightarrow F^j \bar{F}^j$	17
2. $A_L^{\ell,a} A_L^{\ell,a} \rightarrow A_L^{\ell,b} A_L^{\ell,b}$	20
3. $A_L^{\ell,a} A_L^{\ell,b} \rightarrow A_L^{\ell,a} A_L^{\ell,b}$	24
4. $F^i \bar{F}^i \rightarrow A_L^{\ell,a} A_L^{\ell,a}$	25
5. $F^i \bar{F}^j \rightarrow A_L^{\ell,a} A_L^{\ell,b}$	27
IV PARTIAL WAVE UNITARITY CONSTRAINT	29
1. $F^i \bar{F}^i \rightarrow F^j \bar{F}^j$	31
2. $A_L^{\ell,a} A_L^{\ell,a} \rightarrow A_L^{\ell,b} A_L^{\ell,b}$	32

CONTENTS (Continued)

	Page
3. $A_L^{\ell,a} A_L^{\ell,b} \rightarrow A_L^{\ell,a} A_L^{\ell,b}$	36
4. $F^i \bar{F}^i \rightarrow A_L^{\ell,a} A_L^{\ell,a}$	37
5. $F^i \bar{F}^j \rightarrow A_L^{\ell,a} A_L^{\ell,b}$	38
V NEUTRINO SPECTRUM	42
VI NEUTRINO MIXING	48
1. Constraint on neutrino mixing parameter	51
VII CONCLUSION AND DISCUSSIONS	54
REFERENCES	56
APPENDICES	
APPENDIX A STRUCTURE CONSTANTS	60
APPENDIX B $A_L^{\ell,a} A_L^{\ell,a} \rightarrow A_L^{\ell,b} A_L^{\ell,b}$	62
APPENDIX C $A_L^{\ell,a} A_L^{\ell,b} \rightarrow A_L^{\ell,a} A_L^{\ell,b}$	66
CURRICULUM VITAE	69

LIST OF TABLES

Table		Page
2.1	Transformation properties under $SU(2)_L, U(1)_Y, SU(3)_\ell$ and $SU(3)_E$ of SM leptons, flavor-mirror fields, flavons and Higgs field.	4
5.1	Current neutrino data from neutrino oscillation.	42
6.1	The best-fit($\pm 1\sigma$) of three neutrino oscillation from the present experiment neutrino data(Patrignani et al., 2016) and $\sin \theta_{23}$ [NH/IH] from propagating errors (Tanabashi et al., 2018).	52

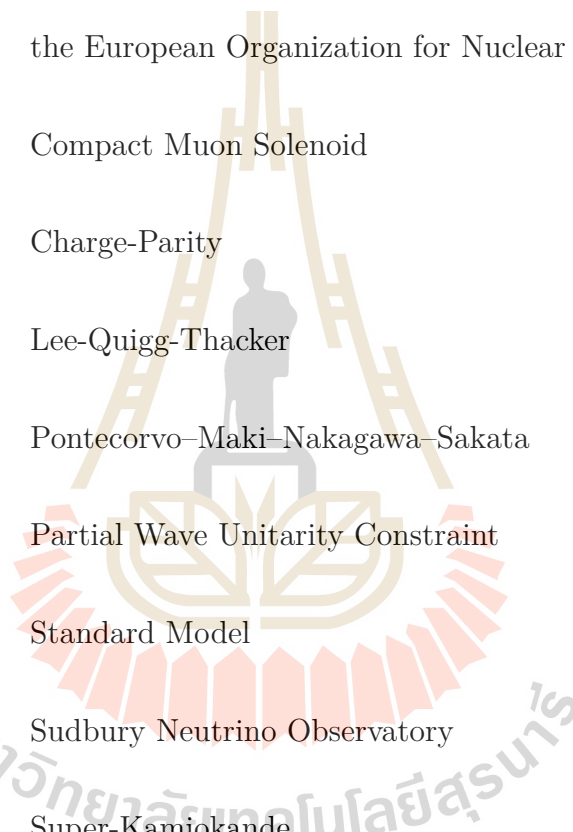


LIST OF FIGURES

Figure		Page
4.1	Boundary of a_j for $AB \rightarrow AB$ process at high energy limit.	30
5.1	Comparison between global convention and this work convention	43
5.2	The region of perturbative unitary bound on neutrino spectrum when $\langle \mathcal{Y}_N \rangle$ is diagonal.	44
5.3	Viable neutrino spectra for normal hierarchy (red). Region com- patible with perturbative unitarity is shown in green.	46
5.4	Scale of neutrino mass squared differences in normal and inverted hierarchy.	47
6.1	Grid chart for scanning mixing parameter when red dots stand for $(\sin \theta_{23})_{ij}$ at $(\sin \theta_{13})_i, (\sin \theta_{12})_j$	52
6.2	Result from scanning mixing parameters in range 2σ . Blue region is the perturbative region. Red line is viable neutrino spectrum for normal hierarchy.	53

LIST OF ABBREVIATIONS

ALICE	A Large Ion Collider Experiment
BSM	Beyond the Standard Model
CERN	the European Organization for Nuclear Research
CMS	Compact Muon Solenoid
CP	Charge-Parity
LQT	Lee-Quigg-Thacker
PMNS	Pontecorvo–Maki–Nakagawa–Sakata
PWUC	Partial Wave Unitarity Constraint
SM	Standard Model
SNO	Sudbury Neutrino Observatory
Super-K	Super-Kamiokande



CHAPTER I

INTRODUCTION

One of the elementary particles which has no charge, spin-1/2 and interacts very weakly with other particles is called the *neutrino*. There are some undetermined properties such as masses and mixing angles that particle physicists want to find out. Neutrino can undergo a quantum phenomenon known as *neutrino oscillation** under which neutrino changes type. This phenomenon was confirmed by the Super-Kamiokande (Super-K) in Japan (Fukuda et al., 1998) and the Sudbury Neutrino Observatory (SNO) in Canada (Ahmad et al., 2001). It implied that neutrino must be a massive particle which is in contradiction with the Standard Model (SM) of particle physics. This is a direct evidence that the SM has to be extended to accommodate a massive neutrino.

From present experimental data the mass of neutrino is very light, $m_\nu < 2$ eV (Tanabashi et al., 2018), much lighter than other particles. There are models that can generate light neutrino mass such as seesaw models which connect the mass of the neutrino with the mass of a heavy new physics particle. There are many realizations of seesaw models (Akhmedov, 2014), each of which depends on additional new heavy particles: type I, II and III corresponding to heavy sterile neutrinos[†], heavy $SU(2)_L$ -triplet Higgs scalars and heavy triplet fermions, respectively.

Another shortcoming of the SM is the lack of explanation of why there

*In 2015, Takaaki Kajita (Super-K) and Arthur B. McDonald (SNO) received the Noble Prize in Physics for a discovery of neutrino oscillation.

[†]One special type of neutrino in the extension of the SM which does not have the SM gauge interactions.

are only three types of lepton flavor. The number of lepton flavors could be explained by Beyond the Standard Model (BSM) physics. In the SM, there is an approximated $SU(3)_l \times SU(3)_E$ symmetry in the lepton sector which is broken by the lepton Yukawa coupling. One could consider BSM scenario in which this symmetry is exact, such as model with gauged lepton flavor symmetry (Alonso et al., 2016). This model explains the number of flavors by equating it to the size of the $SU(3)_l \times SU(3)_E$ representation under which leptons transform. Three extra fermion species were introduced to cancel gauge anomalies. In this model, one of the extra fermion fields can be interpreted as a right-handed neutrino, which can generate small neutrino mass via a seesaw mechanism.

In this work we will study neutrino properties in the framework of gauged lepton flavor symmetry. A theoretical technique called *partial wave unitarity constraint* (PWUC) will be utilized to constrain the mass of flavor gauge bosons. This is achieved by evaluating all possible flavor gauge boson scattering amplitudes. PWUC implies that the amplitude cannot grow arbitrarily large; this places an upper bound on the mass of flavor gauge boson which is inversely proportional to the mass of neutrino.

Then we can evaluate the PWUC in a particular basis by scanning the model parameter space for viable neutrino spectra. To investigate neutrino mixing, the PWUC is obtained in another basis choice. This basis gives mixing parameters encoded in gauge boson mass matrix. Then unitarity perturbative region will be used to constrain a conservative bound of mixing parameter.

This thesis is organized as follows. In chapter I, we review the shortcomings of the SM and how the model with gauged lepton flavor could address them. Then we give an overview of the model in chapter II. It includes the transformation properties, interactions and mass matrices of gauge bosons. These interactions lead

us to evaluate the longitudinal gauge boson scattering amplitudes at tree-level in chapter III. In order to constrain neutrino properties, amplitudes and gauge boson mass will be subjected to the partial wave unitarity constraint technique and we will express them in chapter IV. Next, the results of scanning the model parameter space for viable parameters such as neutrino spectrum and mixing angles will be presented in chapter V and VI respectively. Finally, we conclude the thesis and discuss our results in chapter VII.



CHAPTER II

GAUGED LEPTON FLAVOR MODEL

This chapter presents the $SU(3)_\ell \times SU(3)_E$ gauged lepton flavor model in order to address shortcomings of the SM in the number of lepton families and neutrino masses: Why is the fermion flavor structure the way it is? Why are there three families of quarks and leptons? What is the mechanism behind very light neutrinos? The structure of the model such as transformation properties of all fields, their interactions and flavor gauge boson mass matrix are presented in this chapter respectively.

In this model, lepton flavors are promoted to gauge symmetry. This leads to lepton flavor gauge anomalies. These gauge anomalies can be canceled by introducing three extra fermions, \mathcal{E}_R , \mathcal{E}_L and \mathcal{N}_R . Moreover, one of new fermions acts as a right-handed neutrino which then generates a small neutrino mass. The Yukawa couplings are promoted to scalar fields (flavon fields), \mathcal{Y}_E and \mathcal{Y}_N , which transform under $SU(3)_\ell \times SU(3)_E$ gauge transformation to preserve flavor symmetry. Their transformation properties are listed in Table 2.1.

Table 2.1 Transformation properties under $SU(2)_L, U(1)_Y, SU(3)_\ell$ and $SU(3)_E$ of SM leptons, flavor-mirror fields, flavons and Higgs field.

	$SU(2)_L$	$U(1)_Y$	$SU(3)_\ell$	$SU(3)_E$
$L \equiv (\nu_L, e_L)$	2	-1/2	3	1
e_R	1	-1	1	3
\mathcal{E}_R	1	-1	3	1
\mathcal{E}_L	1	-1	1	3
\mathcal{N}_R	1	0	3	1
\mathcal{Y}_E	1	0	$\bar{3}$	3
\mathcal{Y}_N	1	0	$\bar{6}$	1
H	2	1/2	1	1

1. Interactions

The most general renormalizable Lagrangian for $SU(3)_\ell \times SU(3)_E$ gauge symmetry (Alonso,) is

$$\begin{aligned} \mathcal{L} = & i \sum_{\psi} \bar{\psi} \not{D} \psi - \frac{1}{2} \sum_I \text{Tr} \left(F_{\mu\nu}^I F_I^{\mu\nu} \right) + \sum_B \text{Tr} (D_\mu \mathcal{Y}_B D^\mu \mathcal{Y}_B^\dagger) \\ & + D_\mu H^\dagger D^\mu H + \mathcal{L}_{Yuk} - V(H, \mathcal{Y}_E, \mathcal{Y}_N) \end{aligned} \quad (2.1)$$

where ψ refers to all lepton species in Table 2.1. The indices $I = l, E$ represent lepton indices and $B = E, N$ label flavon indices. For scalar interactions, they are hidden in the scalar potential which is relevant to flavor vevs after flavor symmetry breaking. This potential has been studied by Alonso and his colleagues (Alonso et al., 2012; Alonso et al., 2013a; Alonso et al., 2013b).

The part of the general renormalization Lagrangian relevant for this work is

$$\mathcal{L} \supset i \bar{\psi} \not{D} \psi + \sum_B \text{Tr} (D_\mu \mathcal{Y}_B D^\mu \mathcal{Y}_B^\dagger) + \mathcal{L}_{Yuk} - V(H, \mathcal{Y}_E, \mathcal{Y}_N). \quad (2.2)$$

The covariant derivatives of \mathcal{N}_R , \mathcal{Y}_N , and \mathcal{Y}_E are

$$\begin{aligned} D_\mu \mathcal{N}_R &= (\partial_\mu + i g_\ell A_\mu^\ell) \mathcal{N}_R, \\ D_\mu \mathcal{Y}_N &= \partial_\mu \mathcal{Y}_N - i g_l (A_\mu^\ell)^T \mathcal{Y}_N - i g_\ell \mathcal{Y}_N A_\mu^\ell, \\ D_\mu \mathcal{Y}_E &= \partial_\mu \mathcal{Y}_E - i g_E A_\mu^E \mathcal{Y}_E - i g_\ell \mathcal{Y}_E A_\mu^\ell. \end{aligned} \quad (2.3)$$

Here, A_μ^ℓ and A_μ^E are in $SU(3)$ structure of the form

$$\begin{aligned} A_\mu^\ell &\equiv \sum_{a=1}^8 A_\mu^{\ell,a} T^a, \\ A_\mu^E &\equiv \sum_{a=1}^8 A_\mu^{E,a} T^a, \end{aligned} \quad (2.4)$$

where T^a are the SU(3) generators defined as half of the Gell-Mann matrices, $T^a \equiv \lambda^a/2$. They satisfy $(T^a)_{\alpha\beta} = (T^a)_{\beta\alpha}^*$ and $[T^a, T^b] = if^{abc}T^c$.

Next, we will express the form of gauge boson masses from the gauge Lagrangian after flavor symmetry breaking.

2. Flavor gauge lepton mass

All masses of sixteen gauge bosons are produced after flavor symmetry breaking where the flavor gauge Lagrangian becomes

$$\mathcal{L}_{\text{gauge}} \supset \frac{1}{2} \sum_{I=\ell, E} \text{Tr} \left(F_{\mu\nu}^I F_I^{\mu\nu} \right) + \frac{1}{2} \sum_{a,b=1}^{16} \chi_\mu^a \left(M_A^2 \right)_{ab} \chi^{b,\mu} - \sum_{I=\ell, E} g_I \text{Tr} \left(A_\mu^I J_{A_I}^\mu \right), \quad (2.5)$$

where

$$\chi_\mu \equiv \{ A_\mu^{\ell,1}, \dots, A_\mu^{\ell,8}, A_\mu^{E,1}, \dots, A_\mu^{E,8} \}. \quad (2.6)$$

The lepton currents are

$$[J_{A_\ell}^\mu]_{ij} = \bar{L}^j \gamma^\mu L^i + \bar{\mathcal{E}}_R^j \gamma^\mu \mathcal{E}_R^i + \bar{\mathcal{N}}_R^j \gamma^\mu \mathcal{N}_R^i, \quad (2.7)$$

$$[J_{A_E}^\mu]_{ij} = \bar{e}_R^j \gamma^\mu e_R^i + \bar{\mathcal{E}}_L^j \gamma^\mu \mathcal{E}_L^i,$$

and the mass matrix of the flavor gauge bosons is in block diagonal form

$$\mathcal{M}_A^2 = \begin{pmatrix} M_{\ell\ell}^2 & M_{\ell E}^2 \\ M_{E\ell}^2 & M_{EE}^2 \end{pmatrix} \quad (2.8)$$

where

$$\begin{aligned}
(M_{\ell\ell}^2)_{ab} &= g_\ell^2 \left[\text{Tr} \left(\mathcal{Y}_E \{T^a, T^b\} \mathcal{Y}_E^\dagger \right) + \text{Tr} \left(\mathcal{Y}_N \{T^a, T^b\} \mathcal{Y}_N^\dagger \right) + \text{Tr} \left(\mathcal{Y}_N^\dagger \{T^{aT}, T^{bT}\} \mathcal{Y}_N \right) \right. \\
&\quad \left. + 2 \text{Tr} \left(\mathcal{Y}_N^\dagger T^{aT} \mathcal{Y}_N T^b + \mathcal{Y}_N^\dagger T^{bT} \mathcal{Y}_N T^a \right) \right], \\
(M_{\ell E}^2)_{ab} &= (M_{E\ell}^2)_{ba} = -2g_\ell g_E \text{Tr} \left(T^a \mathcal{Y}_E^\dagger T^b \mathcal{Y}_E \right), \\
(M_{EE}^2)_{ab} &= g_E^2 \text{Tr} \left(\mathcal{Y}_E^\dagger \{T^a, T^b\} \mathcal{Y}_E \right).
\end{aligned} \tag{2.9}$$

Since $\mathcal{Y}_N \gg \mathcal{Y}_E$, $A_\mu^{\ell,a}$ are approximately the heaviest heavy flavor gauge bosons. Then the mass matrix is approximately diagonal by domination of $(M_{\ell\ell})_{ab}$,

$$\begin{aligned}
(M_{\ell\ell}^2)_{ab} &\simeq g_\ell^2 \left[\text{Tr} \left(\mathcal{Y}_N \{T^a, T^b\} \mathcal{Y}_N^\dagger \right) + \text{Tr} \left(\mathcal{Y}_N^\dagger \{T^{aT}, T^{bT}\} \mathcal{Y}_N \right) \right. \\
&\quad \left. + 2 \text{Tr} \left(\mathcal{Y}_N^\dagger T^{aT} \mathcal{Y}_N T^b + \mathcal{Y}_N^\dagger T^{bT} \mathcal{Y}_N T^a \right) \right].
\end{aligned} \tag{2.10}$$

Next, we will show how this gauge boson mass is related to the neutrino mass. To identify lepton mass, the Yukawa interactions relevant to the fermion mass are

$$\begin{aligned}
\mathcal{L}_{Yuk} &= \lambda_E \bar{\ell}_L H \mathcal{E}_R + \mu_E \bar{\mathcal{E}}_L e_R + \lambda_E \bar{\mathcal{E}}_L \mathcal{Y}_E \mathcal{E}_R \\
&\quad + \lambda_\nu \bar{\ell}_L \tilde{H} \mathcal{N}_R + \frac{\lambda_N}{2} \bar{\mathcal{N}}_R^c \mathcal{Y}_N \mathcal{N}_R + \text{h.c.}
\end{aligned} \tag{2.11}$$

After both electroweak and flavor symmetries are broken spontaneously by

background of the scalars

$$H \equiv \frac{1}{\sqrt{2}} \begin{pmatrix} 0 \\ v + h \end{pmatrix}, \quad (2.12)$$

$$\mathcal{Y}_E \equiv \langle \mathcal{Y}_E \rangle + \phi_E / \sqrt{2},$$

$$\mathcal{Y}_N \equiv \langle \mathcal{Y}_N \rangle + \phi_N / \sqrt{2},$$

the mass matrices for the charged and neutral leptons are

$$\begin{pmatrix} 0 & \lambda_E v / \sqrt{2} \\ \mu_E & \lambda_E \langle \mathcal{Y}_E \rangle \end{pmatrix} + \text{h.c.}, \quad \frac{1}{2} \begin{pmatrix} 0 & \lambda_\nu v / \sqrt{2} \\ \lambda_\nu v / \sqrt{2} & \lambda_N \langle \mathcal{Y}_N \rangle \end{pmatrix} + \text{h.c.}, \quad (2.13)$$

where each entry is a 3 by 3 matrix. Both mass matrices are in a typical see-saw form. Taking $\langle \mathcal{Y}_E \rangle \gg v, \mu_E$ and $\langle \mathcal{Y}_N \rangle \gg v$, we find the mass matrices for the light leptons, $m_{l(\nu)}$, and the heavy leptons, $M_{\mathcal{E}(N)}$, satisfy

$$M_{\mathcal{E}} \simeq \lambda_E \langle \mathcal{Y}_E \rangle, \quad m_l M_{\mathcal{E}} \simeq \lambda_E \mu_E v / \sqrt{2}, \quad \text{and} \quad (2.14)$$

$$M_N \simeq \lambda_N \langle \mathcal{Y}_N \rangle, \quad m_\nu M_N \simeq \lambda_\nu^2 v^2 / 2.$$

To directly study the neutrino mass, we work in the basis where $\langle \mathcal{Y}_N \rangle$ is diagonal, we deduce

$$\langle \mathcal{Y}_N \rangle \simeq \frac{\lambda_\nu^2 v}{2\lambda_N} \text{diag} \left(\frac{v}{m_{\nu_1}}, \frac{v}{m_{\nu_2}}, \frac{v}{m_{\nu_3}} \right), \quad (2.15)$$

$$\langle \mathcal{Y}_E \rangle \simeq \frac{\lambda_E \mu_E}{\sqrt{2}\lambda_E} U^\dagger \text{diag} \left(\frac{v}{m_e}, \frac{v}{m_\mu}, \frac{v}{m_\tau} \right) V,$$

where U and V are heavy lepton mixing matrices. Without loss of generality, we take $m_{\nu_1} < m_{\nu_2} < m_{\nu_3}$. Thus $N_1(N_3)$ is the heaviest (lightest) heavy neutrino.

Notice that $\langle \mathcal{Y}_E \rangle$ and $\langle \mathcal{Y}_N \rangle$ cannot be simultaneously diagonalized. Thus, there are two choices of basis which can address on gauge boson mass in (2.10).

First, $\langle \mathcal{Y}_N \rangle$ is selected to be diagonal. This choice produces two heavy lepton mixing matrices, U and V , to $\langle \mathcal{Y}_E \rangle$. The second basis choice is diagonal \mathcal{Y}_E and then the well-known light lepton mixing matrix, the PMNS matrix, will be encoded in \mathcal{Y}_N .

The mass matrix of the $A_\mu^{\ell,a}$ gauge boson in the limit $\langle \mathcal{Y}_E \rangle \gg \langle \mathcal{Y}_N \rangle$ is

$$M_{\ell\ell}^2 = \begin{pmatrix} M_{11} & 0 & 0 & 0 & 0 & 0 & 0 & 0 \\ 0 & M_{22} & 0 & 0 & 0 & 0 & 0 & 0 \\ 0 & 0 & M_{33} & 0 & 0 & 0 & 0 & M_{38} \\ 0 & 0 & 0 & M_{44} & 0 & 0 & 0 & 0 \\ 0 & 0 & 0 & 0 & M_{55} & 0 & 0 & 0 \\ 0 & 0 & 0 & 0 & 0 & M_{66} & 0 & 0 \\ 0 & 0 & 0 & 0 & 0 & 0 & M_{77} & 0 \\ 0 & 0 & M_{83} & 0 & 0 & 0 & 0 & M_{88} \end{pmatrix}, \quad (2.16)$$

where matrix elements in unit of $g_\ell^2 (\frac{\lambda_\nu^2 v}{2\lambda_N m_{\nu_3}})^2$ are

$$\begin{aligned}
M_{11} &= (x + y)^2, \\
M_{22} &= (x - y)^2, \\
M_{44} &= (x + 1)^2, \\
M_{55} &= (x - 1)^2, \\
M_{66} &= (y + 1)^2, \\
M_{77} &= (y - 1)^2, \\
M_{33} &= 2(x^2 + y^2), \\
M_{88} &= \frac{2}{3}(x^2 + y^2 + 4), \\
M_{38} &= \frac{2}{\sqrt{3}}(x - y)(x + y), \\
M_{83} &= \frac{2}{\sqrt{3}}(x - y)(x + y),
\end{aligned} \tag{2.17}$$

and $x \equiv m_{\nu_3}/m_{\nu_1}$, $y \equiv m_{\nu_3}/m_{\nu_2}$.

Notice that the third and eighth components are not in mass eigenstates.

In order to handle them, we write their elements into a 2×2 matrix

$$M_{\pm}^2 = \begin{pmatrix} M_{33} & M_{38} \\ M_{83} & M_{88} \end{pmatrix}, \tag{2.18}$$

and diagonalize it by mixing flavor eigenstates. Let

$$\begin{pmatrix} A_\mu^{\ell,3} \\ A_\mu^{\ell,8} \end{pmatrix} = \begin{pmatrix} c_\alpha & -s_\alpha \\ s_\alpha & c_\alpha \end{pmatrix} \begin{pmatrix} A_\mu^{\ell,-} \\ A_\mu^{\ell,+} \end{pmatrix}, \tag{2.19}$$

then substitute it into term of flavor gauge boson mass, $A_\mu^{\ell,a}$,

$$\begin{aligned}
& \begin{pmatrix} A_\mu^{\ell,3} & A_\mu^{\ell,8} \end{pmatrix} M_\pm^2 \begin{pmatrix} A_\mu^{\ell,3} \\ A_\mu^{\ell,8} \end{pmatrix} \\
&= \begin{pmatrix} A_\mu^{\ell,-} & A_\mu^{\ell,+} \end{pmatrix} \begin{pmatrix} c_\alpha & s_\alpha \\ -s_\alpha & c_\alpha \end{pmatrix} \begin{pmatrix} M_{33} & M_{38} \\ M_{83} & M_{88} \end{pmatrix} \begin{pmatrix} c_\alpha & -s_\alpha \\ s_\alpha & c_\alpha \end{pmatrix} \begin{pmatrix} A_\mu^{\ell,-} \\ A_\mu^{\ell,+} \end{pmatrix}, \quad (2.20) \\
&= \begin{pmatrix} A_\mu^{\ell,-} & A_\mu^{\ell,+} \end{pmatrix} \hat{M}_\pm^2 \begin{pmatrix} A_\mu^{\ell,-} \\ A_\mu^{\ell,+} \end{pmatrix},
\end{aligned}$$

where

$$\hat{M}_\pm^2 = \begin{pmatrix} M_{33}^\pm & M_{38}^\pm \\ M_{83}^\pm & M_{88}^\pm \end{pmatrix}, \quad (2.21)$$

and

$$\begin{aligned}
M_{33}^\pm &= M_{33}c_\alpha^2 + 2M_{83}s_\alpha c_\alpha + M_{88}s_\alpha^2 \\
M_{38}^\pm &= M_{83}c_\alpha^2 - M_{33}s_\alpha c_\alpha + M_{88}s_\alpha c_\alpha - M_{83}s_\alpha^2 \\
M_{83}^\pm &= M_{83}c_\alpha^2 - M_{33}s_\alpha c_\alpha + M_{88}s_\alpha c_\alpha - M_{83}s_\alpha^2 \\
M_{88}^\pm &= M_{88}c_\alpha^2 - 2M_{83}s_\alpha c_\alpha + M_{33}s_\alpha^2
\end{aligned} \quad (2.22)$$

$$s_\alpha = \sqrt{\frac{1}{2} + \frac{x^2 + y^2 - 2}{4\sqrt{x^4 + y^4 - x^2y^2 - x^2 - y^2 + 1}}}, \quad (2.23)$$

$$c_\alpha = \sqrt{\frac{1}{2} - \frac{x^2 + y^2 - 2}{4\sqrt{x^4 + y^4 - x^2y^2 - x^2 - y^2 + 1}}}.$$

Finally, the $A_\mu^{\ell,a}$ mass matrix gives pairwise eigenvalues,

$$\begin{aligned}
\hat{M}_{A^1}^2 &= \hat{M}_{A^2}^2 + 4xy = x^2 + y^2 + 2xy, \\
\hat{M}_{A^4}^2 &= \hat{M}_{A^5}^2 + 4x = x^2 + 2x + 1, \\
\hat{M}_{A^6}^2 &= \hat{M}_{A^7}^2 + 4y = y^2 + 2y + 1, \\
\hat{M}_{A^\pm}^2 &= \frac{4}{3} \left(x^2 + y^2 + 1 \pm \sqrt{x^4 + y^4 - x^2y^2 - x^2 - y^2 + 1} \right),
\end{aligned} \tag{2.24}$$

where $A_\mu^{\ell,\pm}$ are mass eigenstates in the unit of $\frac{g_l^2 v^4 \lambda_\nu^4}{4\lambda_N^2 m_{\nu_3}^2}$ with

$$\begin{pmatrix} A_\mu^{\ell,-} \\ A_\mu^{\ell,+} \end{pmatrix} = \begin{pmatrix} c_\alpha & s_\alpha \\ -s_\alpha & c_\alpha \end{pmatrix} \begin{pmatrix} A_\mu^{\ell,3} \\ A_\mu^{\ell,8} \end{pmatrix}. \tag{2.25}$$

Now, we have related the masses of flavor gauge bosons to three neutrino masses. In the next chapter, we will calculate the scattering amplitude for various processes where gauge boson masses will be involved.

CHAPTER III

SCATTERING AMPLITUDES

In this chapter we will evaluate the scattering amplitudes which potentially can grow with center of mass energy. There are five processes at tree-level: $F^i \bar{F}^i \rightarrow F^j \bar{F}^j$, $A_L^{\ell,a} A_L^{\ell,a} \rightarrow A_L^{\ell,b} A_L^{\ell,b}$, $A_L^{\ell,a} A_L^{\ell,b} \rightarrow A_L^{\ell,a} A_L^{\ell,b}$, $F^i \bar{F}^j \rightarrow A_L^{\ell,a} A_L^{\ell,b}$ and $F^i \bar{F}^i \rightarrow A_L^{\ell,a} A_L^{\ell,a}$. We will start by listing all ingredients for calculating Feynman diagrams. Then, we will examine which scattering amplitudes are able to constrain neutrino mass by partial wave unitary technique. Note that all interactions and couplings come from the Lagrangian of the model with gauged lepton flavor.

Ingredients for scattering amplitudes:

The simplest calculation assumes that two incoming(outgoing) particles are identical. We can write 4-momenta of the particles as

$$\begin{aligned}
 p_1 &= (\sqrt{s}/2, 0, 0, p), \\
 p_2 &= (\sqrt{s}/2, 0, 0, -p), \\
 p_3 &= (\sqrt{s}/2, p\sqrt{1-x^2}, 0, px), \\
 p_4 &= (\sqrt{s}/2, -p\sqrt{1-x^2}, 0, -px),
 \end{aligned} \tag{3.1}$$

where $x \equiv \cos(\theta)$. We take p_1, p_2 (p_3, p_4) to be momenta of the incoming (outgoing)

particles. Mandelsalam's variable are given by

$$\begin{aligned}
 s &= (p_1 + p_2)^2 = (2\sqrt{s})^2 = 4s = E_{cm}^2, \\
 t &= (p_1 - p_3)^2 = -2p^2(x - 1), \\
 u &= (p_1 - p_4)^2 = -2p^2(x + 1),
 \end{aligned} \tag{3.2}$$

where E_{cm} is the center of mass energy.

For processes $F^i \bar{F}^i \rightarrow F^j \bar{F}^j$ and $F^i \bar{F}^i \rightarrow A_L^{l,a} A_L^{l,a}$, there are two incoming fermions. Their spin properties should be considered as well. By solving Dirac equation, there are four independent spinor bases

$$\xi_1 = \begin{pmatrix} 1 \\ 0 \end{pmatrix}, \quad \xi_2 = \begin{pmatrix} 0 \\ 1 \end{pmatrix}, \quad \xi_3 = \begin{pmatrix} \frac{\sqrt{1+x}}{2} \\ \frac{\sqrt{1-x}}{2} \end{pmatrix}, \quad \xi_4 = \begin{pmatrix} \frac{-\sqrt{1-x}}{2} \\ \frac{\sqrt{1+x}}{2} \end{pmatrix}. \tag{3.3}$$

Typically, the forms of the spinor are

$$\begin{aligned}
 u(p_1) = u_1 &= \begin{pmatrix} \sqrt{p_1 \cdot \sigma} \xi_1 \\ \sqrt{p_1 \cdot \bar{\sigma}} \xi_1 \end{pmatrix}, & v(p_1) = v_1 &= \begin{pmatrix} \sqrt{p_1 \cdot \sigma} \xi_1 \\ -\sqrt{p_1 \cdot \bar{\sigma}} \xi_1 \end{pmatrix}, \\
 u(p_2) = u_2 &= \begin{pmatrix} \sqrt{p_2 \cdot \sigma} \xi_2 \\ \sqrt{p_2 \cdot \bar{\sigma}} \xi_2 \end{pmatrix}, & v(p_2) = v_2 &= \begin{pmatrix} \sqrt{p_2 \cdot \sigma} \xi_2 \\ -\sqrt{p_2 \cdot \bar{\sigma}} \xi_2 \end{pmatrix}, \\
 u(p_3) = u_3 &= \begin{pmatrix} \sqrt{p_3 \cdot \sigma} \xi_3 \\ \sqrt{p_3 \cdot \bar{\sigma}} \xi_3 \end{pmatrix}, & v(p_3) = v_3 &= \begin{pmatrix} \sqrt{p_3 \cdot \sigma} \xi_3 \\ -\sqrt{p_3 \cdot \bar{\sigma}} \xi_3 \end{pmatrix}, \\
 u(p_4) = u_4 &= \begin{pmatrix} \sqrt{p_4 \cdot \sigma} \xi_4 \\ \sqrt{p_4 \cdot \bar{\sigma}} \xi_4 \end{pmatrix}, & v(p_4) = v_4 &= \begin{pmatrix} \sqrt{p_4 \cdot \sigma} \xi_4 \\ -\sqrt{p_4 \cdot \bar{\sigma}} \xi_4 \end{pmatrix},
 \end{aligned} \tag{3.4}$$

where σ is Pauli matrix. The general fermion spinors are

$$\begin{aligned}
u_1 &= \begin{pmatrix} \sqrt{\frac{\sqrt{s}}{2} - p} \\ 0 \\ \sqrt{\frac{\sqrt{s}}{2} + p} \\ 0 \end{pmatrix}, \quad \bar{u}_1 = \begin{pmatrix} \sqrt{\frac{\sqrt{s}}{2} + p} \\ 0 \\ \sqrt{\frac{\sqrt{s}}{2} - p} \\ 0 \end{pmatrix}^T, \\
u_2 &= \begin{pmatrix} 0 \\ \sqrt{\frac{\sqrt{s}}{2} - p} \\ 0 \\ \sqrt{\frac{\sqrt{s}}{2} + p} \end{pmatrix}, \quad \bar{u}_2 = \begin{pmatrix} 0 \\ \sqrt{\frac{\sqrt{s}}{2} + p} \\ 0 \\ \sqrt{\frac{\sqrt{s}}{2} - p} \end{pmatrix}^T, \\
u_3 &= \frac{1}{\sqrt{2}} \begin{pmatrix} \sqrt{1+x}\sqrt{\frac{\sqrt{s}}{2}-p} \\ \sqrt{1-x}\sqrt{\frac{\sqrt{s}}{2}-p} \\ \sqrt{1+x}\sqrt{\frac{\sqrt{s}}{2}+p} \\ \sqrt{1-x}\sqrt{\frac{\sqrt{s}}{2}+p} \end{pmatrix}, \quad \bar{u}_3 = \frac{1}{\sqrt{2}} \begin{pmatrix} \sqrt{1+x}\sqrt{\frac{\sqrt{s}}{2}+p} \\ \sqrt{1-x}\sqrt{\frac{\sqrt{s}}{2}+p} \\ \sqrt{1+x}\sqrt{\frac{\sqrt{s}}{2}-p} \\ \sqrt{1-x}\sqrt{\frac{\sqrt{s}}{2}-p} \end{pmatrix}^T, \\
u_4 &= \frac{1}{\sqrt{2}} \begin{pmatrix} \sqrt{1-x}\sqrt{\frac{\sqrt{s}}{2}-p} \\ -\sqrt{1+x}\sqrt{\frac{\sqrt{s}}{2}-p} \\ -\sqrt{1-x}\sqrt{\frac{\sqrt{s}}{2}+p} \\ \sqrt{1+x}\sqrt{\frac{\sqrt{s}}{2}+p} \end{pmatrix}, \quad \bar{u}_4 = \frac{1}{\sqrt{2}} \begin{pmatrix} -\sqrt{1-x}\sqrt{\frac{\sqrt{s}}{2}+p} \\ \sqrt{1+x}\sqrt{\frac{\sqrt{s}}{2}+p} \\ -\sqrt{1-x}\sqrt{\frac{\sqrt{s}}{2}-p} \\ \sqrt{1+x}\sqrt{\frac{\sqrt{s}}{2}-p} \end{pmatrix}^T,
\end{aligned} \tag{3.5}$$

$$\begin{aligned}
v_1 &= \begin{pmatrix} \sqrt{\frac{\sqrt{s}}{2} - p} \\ 0 \\ -\sqrt{\frac{\sqrt{s}}{2} + p} \\ 0 \end{pmatrix}, & \bar{v}_1 &= \begin{pmatrix} -\sqrt{\frac{\sqrt{s}}{2} + p} \\ 0 \\ \sqrt{\frac{\sqrt{s}}{2} - p} \\ 0 \end{pmatrix}^T, \\
v_2 &= \begin{pmatrix} 0 \\ \sqrt{\frac{\sqrt{s}}{2} - p} \\ 0 \\ -\sqrt{\frac{\sqrt{s}}{2} + p} \end{pmatrix}, & \bar{v}_2 &= \begin{pmatrix} 0 \\ -\sqrt{\frac{\sqrt{s}}{2} + p} \\ 0 \\ \sqrt{\frac{\sqrt{s}}{2} - p} \end{pmatrix}^T, \\
v_3 &= \frac{1}{\sqrt{2}} \begin{pmatrix} \sqrt{1+x}\sqrt{\frac{\sqrt{s}}{2}-p} \\ \sqrt{1-x}\sqrt{\frac{\sqrt{s}}{2}-p} \\ -\sqrt{1+x}\sqrt{\frac{\sqrt{s}}{2}+p} \\ -\sqrt{1-x}\sqrt{\frac{\sqrt{s}}{2}+p} \end{pmatrix}, & \bar{v}_3 &= \frac{1}{\sqrt{2}} \begin{pmatrix} -\sqrt{1+x}\sqrt{\frac{\sqrt{s}}{2}+p} \\ -\sqrt{1-x}\sqrt{\frac{\sqrt{s}}{2}+p} \\ \sqrt{1+x}\sqrt{\frac{\sqrt{s}}{2}-p} \\ \sqrt{1-x}\sqrt{\frac{\sqrt{s}}{2}-p} \end{pmatrix}^T, \\
v_4 &= \frac{1}{\sqrt{2}} \begin{pmatrix} -\sqrt{1-x}\sqrt{\frac{\sqrt{s}}{2}-p} \\ \sqrt{1+x}\sqrt{\frac{\sqrt{s}}{2}-p} \\ \sqrt{1-x}\sqrt{\frac{\sqrt{s}}{2}+p} \\ -\sqrt{1+x}\sqrt{\frac{\sqrt{s}}{2}+p} \end{pmatrix}, & \bar{v}_4 &= \frac{1}{\sqrt{2}} \begin{pmatrix} \sqrt{1-x}\sqrt{\frac{\sqrt{s}}{2}+p} \\ -\sqrt{1+x}\sqrt{\frac{\sqrt{s}}{2}+p} \\ \sqrt{1-x}\sqrt{\frac{\sqrt{s}}{2}-p} \\ \sqrt{1+x}\sqrt{\frac{\sqrt{s}}{2}-p} \end{pmatrix}^T,
\end{aligned} \tag{3.6}$$

where \sqrt{s} is center of mass energy and $\bar{u}(p_i)$ is defined as $u(p_i)\gamma^0$. $u_i(v_i)$ is an incoming fermion(anti-fermion) with momentum p_i . $\bar{u}_i(\bar{v}_i)$ is outgoing fermion(anti-fermion) with momentum p_i .

To relate all variables in the energy form, we will translate them in term of

center of mass energy, For example in $F^i \bar{F}^i \rightarrow F^j \bar{F}^j$, we substitute

$$\begin{aligned}
 p &= \sqrt{\frac{s}{4} - m_f^2} \\
 t &= -\left(\frac{s}{2} - 2m_f^2\right)(1 - x) \\
 u &= -\left(\frac{s}{2} - 2m_f^2\right)(1 + x)
 \end{aligned} \tag{3.7}$$

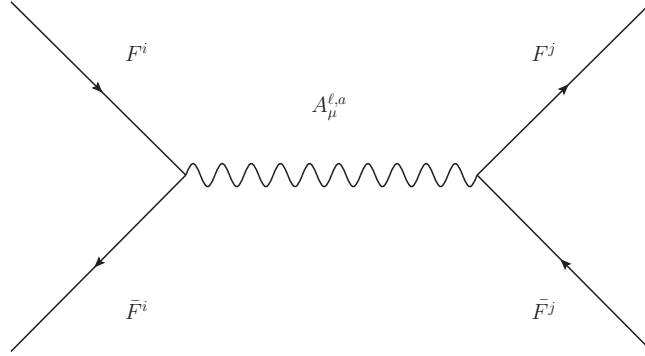
where m_f is an incoming fermion mass and $x = \cos \theta$.

1. $F^i \bar{F}^i \rightarrow F^j \bar{F}^j$

In this model flavor gauge bosons interact with the extra fermions. One of the three extra fermions is of interest in this work because it has the same properties as the right-handed neutrino. Due to gauge freedom, we can choose to calculate in unitary gauge. We will focus on the amplitudes where gauge bosons are being exchanged. Gauge invariance ensures that high energy behavior of the full amplitude obeys unitarity.

Due to the $SU(3)_\ell$ flavor structure, we have 8 gauge bosons together with $SU(3)$ flavor group generator T^a . These gauge bosons can interact with fermions and anti-fermions. Thus all possible processes are $l_L^i \bar{l}_L^i \rightarrow l_L^j \bar{l}_L^j$ and $\mathcal{E}_R^i \bar{\mathcal{E}}_R^i \rightarrow \mathcal{E}_R^j \bar{\mathcal{E}}_R^j$. However, this work focuses only on the light neutrinos. So the process $F^i \bar{F}^i \rightarrow F^j \bar{F}^j$ represents the light neutrino scatterings where i and j are flavor indices.

s-channel:



$$i\mathcal{M}_{A_\mu^a:s\text{-channel}} = (-ig_l T_{ij}^a)^2 \bar{v}_2^i \gamma^\mu \frac{1 - \gamma^5}{2} u_1^j \frac{i}{s - M_A^2} (g^{\mu\nu} - \frac{(p_1 + p_2)^\mu}{M_A^2}) \bar{u}_3^i \gamma_\nu \frac{1 - \gamma^5}{2} v_4^j,$$

$$\mathcal{M}_{A_\mu^a:s\text{-channel}} = - (g_l T_{ij}^a)^2 \frac{-1}{s - M_A^2} (\bar{v}_2^i \gamma^0 \frac{1 - \gamma^5}{2} u_1^j \bar{u}_3^i \gamma^0 \frac{1 - \gamma^5}{2} v_4^j$$

$$- \bar{v}_2^i \gamma^1 \frac{1 - \gamma^5}{2} u_1^j \bar{u}_3^i \gamma^1 \frac{1 - \gamma^5}{2} v_4^j$$

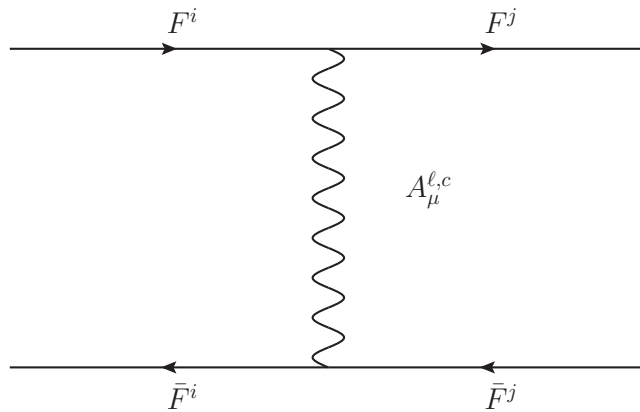
$$- \bar{v}_2^i \gamma^2 \frac{1 - \gamma^5}{2} u_1^j \bar{u}_3^i \gamma^2 \frac{1 - \gamma^5}{2} v_4^j$$

$$- \bar{v}_2^i \gamma^3 \frac{1 - \gamma^5}{2} u_1^j \bar{u}_3^i \gamma^3 \frac{1 - \gamma^5}{2} v_4^j),$$

$$\mathcal{M}_{A_\mu^a:s\text{-channel}} = - (g_l T_{ij}^a)^2 \frac{(x+1)(\sqrt{s} + \sqrt{s - 4m_f^2})^2}{4(s - M_A^2)}.$$

(3.8)

t-channel:



$$i\mathcal{M}_{A_\ell^a:t\text{-channel}} = (-ig_l T_{ij}^a)^2 \bar{v}_2^i \gamma^\mu \frac{1-\gamma^5}{2} v_4^j \frac{i}{t-M_A^2} (g^{\mu\nu} - \frac{(p_1-p_3)^\mu}{M_A^2}) \bar{u}_3^i \gamma_\nu \frac{1-\gamma^5}{2} u_1^j,$$

$$\mathcal{M}_{A_\ell^a:t\text{-channel}} = - (g_l T_{ij}^a)^2 \frac{-1}{t-M_A^2} \left(\bar{v}_2^i \gamma^0 \frac{1-\gamma^5}{2} v_4^j \bar{u}_3^i \gamma^0 \frac{1-\gamma^5}{2} u_1^j \right.$$

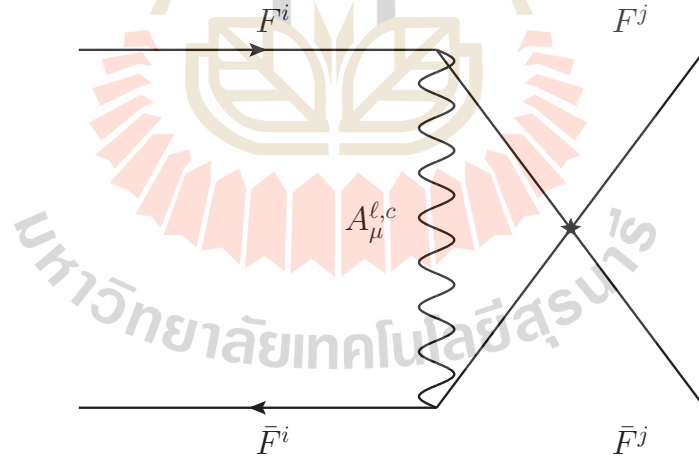
$$\left. - \bar{v}_2^i \gamma^1 \frac{1-\gamma^5}{2} u_1^j \bar{u}_3^i \gamma^1 \frac{1-\gamma^5}{2} v_4^j \right.$$

$$\left. - \bar{v}_2^i \gamma^2 \frac{1-\gamma^5}{2} u_1^j \bar{u}_3^i \gamma^2 \frac{1-\gamma^5}{2} v_4^j \right.$$

$$\left. - \bar{v}_2^i \gamma^3 \frac{1-\gamma^5}{2} u_1^j \bar{u}_3^i \gamma^3 \frac{1-\gamma^5}{2} v_4^j \right),$$

$$\mathcal{M}_{A_\ell^a:t\text{-channel}} = - (g_l T_{ij}^a)^2 \frac{(x+1)(\sqrt{s} + \sqrt{s-4m_f^2})^2}{4M_A^2 + 2(1-x)(s-4m_f^2)}.$$

(3.9)

u-channel:

$$\begin{aligned}
i\mathcal{M}_{A_\ell^a:\text{u-channel}} &= (-ig_l T_{ij}^a)^2 \bar{v}_2^i \gamma^\mu \frac{1-\gamma^5}{2} v_3^j \frac{i}{u-M_A^2} (g^{\mu\nu} - \frac{(p_1-p_4)^\mu}{M_A^2}) \bar{u}_4^i \gamma_\nu \frac{1-\gamma^5}{2} u_1^j, \\
\mathcal{M}_{A_\ell^a:\text{u-channel}} &= - (g_l T_{ij}^a)^2 \frac{-1}{u-M_A^2} \left(\bar{v}_2^i \gamma^0 \frac{1-\gamma^5}{2} u_1^j \bar{u}_3^i \gamma^0 \frac{1-\gamma^5}{2} v_4^j \right. \\
&\quad - \bar{v}_2^i \gamma^1 \frac{1-\gamma^5}{2} v_3^j \bar{u}_4^i \gamma^1 \frac{1-\gamma^5}{2} u_1^j \\
&\quad - \bar{v}_2^i \gamma^2 \frac{1-\gamma^5}{2} v_3^j \bar{u}_4^i \gamma^2 \frac{1-\gamma^5}{2} u_1^j \\
&\quad \left. - \bar{v}_2^i \gamma^3 \frac{1-\gamma^5}{2} v_3^j \bar{u}_4^i \gamma^3 \frac{1-\gamma^5}{2} u_1^j \right), \\
\mathcal{M}_{A_\ell^a:\text{u-channel}} &= - (g_l T_{ij}^a)^2 \frac{(x-1)(\sqrt{s} + \sqrt{s-4m_f^2})^2}{4M_A^2 + 2(1+x)(s-4m_f^2)}.
\end{aligned} \tag{3.10}$$

2. $A_L^{\ell,a} A_L^{\ell,a} \rightarrow A_L^{\ell,b} A_L^{\ell,b}$

This process has identical incoming (outgoing) gauge bosons with momenta k_1, k_2 (p_1, p_2) and mass M_a (M_b). We focus on the longitudinal component of both gauge bosons. Thus, these gauge bosons are in longitudinal polarization states under condition $\epsilon_{p_i} \cdot p_i = 0$. Note that this process is a simple choice of flavor interaction and adequate for our perturbative constraint.

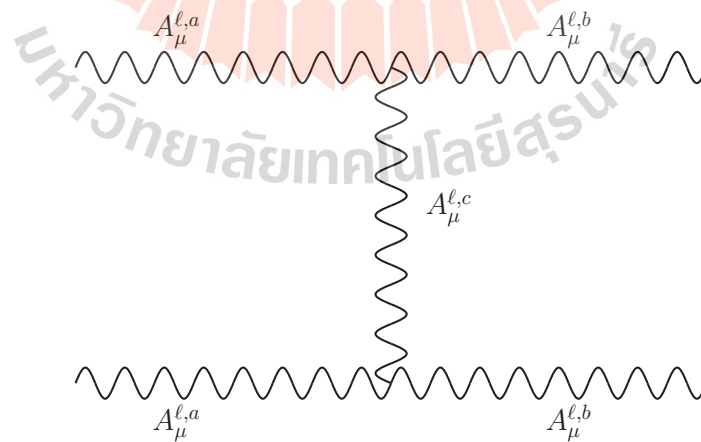
For process $A_L^{\ell,a} A_L^{\ell,a} \rightarrow A_L^{\ell,b} A_L^{\ell,b}$, there are four polarization vectors in longitudinal mode which satisfy $\epsilon(p_i) \cdot p_i = 0$,

$$\begin{aligned}
\epsilon_1 &= \frac{1}{M_{A^a}}(p_i, 0, 0, \frac{\sqrt{s}}{2}), \\
\epsilon_2 &= \frac{1}{M_{A^a}}(p_i, 0, 0, -\frac{\sqrt{s}}{2}), \\
\epsilon_3 &= \frac{1}{M_{A^b}}(p_f, \frac{\sqrt{s}}{2}(1-x^2), 0, \frac{\sqrt{sx}}{2}), \\
\epsilon_4 &= \frac{1}{M_{A^b}}(p_f, -\frac{\sqrt{s}}{2}(1-x^2), 0, -\frac{\sqrt{sx}}{2}).
\end{aligned} \tag{3.11}$$

First, let consider the amplitude with gauge boson exchange in the s-channel, where $A_L^{\ell,c}$ is the intermediate gauge boson. The vertex factor is $f_{aac} \cdot f_{bbc}$ which vanishes by commutation of their group generators. Therefore we do not have the s-channel for $A_L^{\ell,a} A_L^{\ell,a} \rightarrow A_L^{\ell,b} A_L^{\ell,b}$.

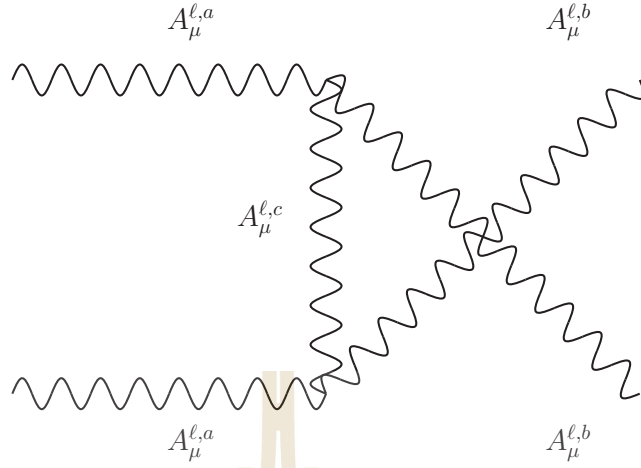
Now, let's carefully consider the amplitude in t- and u- channel. Obviously, their vertex factors do not vanish. Note that there are eight flavor gauge bosons and their flavor interactions are encoded in structure constant.

t-channel:



$$\begin{aligned}
i\mathcal{M}_{A_L^{\ell,c};t\text{-channel}} &= \epsilon_{k_1,\mu}\epsilon_{k_2,\nu}\epsilon_{p_1,\alpha}^*\epsilon_{p_2,\beta}^* \\
&\quad (-ig_A f^{abc}) \left(g^{\mu\lambda}((k_1 - p_1) + k_1)^\alpha + g^{\lambda\alpha}(p_1 - (k_1 - p_1))^\mu \right. \\
&\quad \left. + g^{\alpha\mu}(-k_1 - p_1)^\lambda \right) \\
&\quad \frac{i}{t - M_c^2} \left(g^{\lambda\rho} - \frac{1}{M_c^2} (k_1 - p_1)^\lambda (p_2 - k_2)^\rho \right) \\
&\quad (-ig_A f^{abc}) \left(g^{\nu\beta}(k_2 + p_2)^\rho + g^{\beta\rho}(-p_2 - (p_2 - k_2))^\nu \right. \\
&\quad \left. + g^{\rho\nu}((p_2 - k_2) - k_2)^\beta \right), \\
\mathcal{M}_{A_L^{\ell,c};t\text{-channel}} &= \epsilon_{k_1,\mu}\epsilon_{k_2,\nu}\epsilon_{p_1,\alpha}^*\epsilon_{p_2,\beta}^* \\
&\quad (-ig_A f^{abc})^2 \left(g^{\mu\alpha}(k_1 + p_1)^\lambda + g^{\alpha\lambda}(k_1 - 2p_1)^\mu + g^{\lambda\mu}(p_1 - 2k_1)^\alpha \right) \\
&\quad \frac{1}{t - M_c^2} \left(g^{\lambda\rho} - \frac{1}{M_c^2} (k_1 - p_1)^\lambda (p_2 - k_2)^\rho \right) \\
&\quad \left(g^{\nu\beta}(k_2 + p_2)^\rho + g^{\beta\rho}(k_2 - 2p_2)^\nu + g^{\rho\nu}(p_2 - 2k_2)^\beta \right).
\end{aligned} \tag{3.12}$$

u-channel:



$$\begin{aligned}
 i\mathcal{M}_{A_L^{\ell,c}:u\text{-channel}} &= \epsilon_{k_1,\mu}\epsilon_{k_2,\nu}\epsilon_{p_1,\alpha}^*\epsilon_{p_2,\beta}^* \\
 &(-ig_A f^{abc})\left(g^{\mu\beta}(k_1+p_2)^\lambda + g^{\beta\lambda}(-p_2+(k_1-p_2))^\mu\right. \\
 &\quad \left.+ g^{\lambda\mu}(-(k_1-p_2)-k_1)^\beta\right) \\
 &\frac{i}{u-M_c^2}\left(g^{\lambda\rho} - \frac{1}{M_c^2}(k_1-p_2)^\lambda(p_1-k_2)^\rho\right) \\
 &(-ig_A f^{abc})\left(g^{\nu\alpha}(k_2+p_1)^\rho + g^{\alpha\rho}(-p_1-(p_1-k_2))^\nu\right. \\
 &\quad \left.+ g^{\rho\nu}(k_2-(p_1-k_2))^\alpha\right),
 \end{aligned}$$

$$\begin{aligned}
 \mathcal{M}_{A_L^{\ell,c}:u\text{-channel}} &= \epsilon_{k_1,\mu}\epsilon_{k_2,\nu}\epsilon_{p_1,\alpha}^*\epsilon_{p_2,\beta}^* \\
 &(-ig_A f^{abc})^2\left(g^{\mu\beta}(k_1+p_2)^\lambda + g^{\beta\lambda}(k_1-2p_2)^\mu + g^{\lambda\mu}(p_2-2k_1)^\beta\right) \\
 &\frac{1}{u-M_c^2}\left(g^{\lambda\rho} - \frac{1}{M_c^2}(k_1-p_2)^\lambda(p_1-k_2)^\rho\right) \\
 &\left(g^{\nu\alpha}(k_2+p_1)^\rho + g^{\alpha\rho}(k_2-2p_1)^\nu + g^{\rho\nu}(p_1-2k_2)^\alpha\right).
 \end{aligned}$$

(3.13)

Note that their scalar products will be shown in Appendix B.

$$\mathbf{3.} \quad A_L^{\ell,a} A_L^{\ell,b} \rightarrow A_L^{\ell,a} A_L^{\ell,b}$$

For process $A_L^{\ell,a} A_L^{\ell,b} \rightarrow A_L^{\ell,a} A_L^{\ell,b}$, there are four polarization vectors in longitudinal mode which satisfy $\epsilon(p_i) \cdot p_i = 0$,

$$\begin{aligned} \epsilon_1 &= \frac{1}{M_{A^a}}(p_i, 0, 0, E_1), \\ \epsilon_2 &= \frac{1}{M_{A^b}}(p_i, 0, 0, E_2), \\ \epsilon_3 &= \frac{1}{M_{A^a}}(p_f, 0, E_3\sqrt{(1-x^2)}, E_3x), \\ \epsilon_4 &= \frac{1}{M_{A^b}}(p_f, 0, -E_4\sqrt{(1-x^2)}, -E_4x), \end{aligned} \tag{3.14}$$

and 4-momenta are

$$\begin{aligned} p_1 &= (E_1, 0, 0, p_i), \\ p_2 &= (E_2, 0, 0, -p_i), \\ p_3 &= (E_3, p_f\sqrt{1-x^2}, 0, p_fx), \\ p_4 &= (E_4, -p_f\sqrt{1-x^2}, 0, -p_fx), \end{aligned} \tag{3.15}$$

where $E_1^2 = p_i^2 + M_a^2$, $E_2^2 = p_i^2 + M_b^2$, $E_3^2 = p_j^2 + M_a^2$ and $E_4^2 = p_j^2 + M_b^2$.

For amplitude in t-channel of this process, we will calculate all products in the same way we did for $A_L^{\ell,a} A_L^{\ell,a} \rightarrow A_L^{\ell,b} A_L^{\ell,b}$ t-channel amplitude. In contrary to $A_L^{\ell,a} A_L^{\ell,a} \rightarrow A_L^{\ell,b} A_L^{\ell,b}$, this process does not have amplitude in u-channel but has nonvanishing s-channel one.

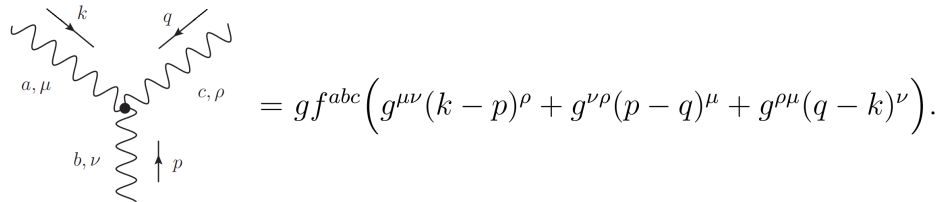
s-channel:

$$\begin{aligned}
i\mathcal{M}_{A_L^{\ell,c}:\text{s-channel}} &= \epsilon_{k_1,\mu}\epsilon_{k_2,\nu}\epsilon_{p_1,\alpha}^*\epsilon_{p_2,\beta}^* \\
&\quad (-ig_A f^{abc}) \left(g^{\mu\lambda}((k_1 + k_2) + k_1)^\nu + g^{\lambda\nu}(-k_2 - (k_1 + k_2))^\mu \right. \\
&\quad \left. + g^{\nu\mu}(-k_1 + k_2)^\lambda \right) \frac{i}{s - M_c^2} \left(g^{\lambda\rho} - \frac{1}{M_c^2} (k_1 + k_2)^\lambda (p_1 + p_2)^\rho \right) \\
&\quad (-ig_A f^{abc}) \left(g^{\alpha\beta}(-p_1 + p_2)^\rho + g^{\beta\rho}(-p_2 - (p_1 + p_2))^\alpha \right. \\
&\quad \left. + g^{\rho\alpha}((p_1 + p_2) + p_1)^\beta \right), \\
\mathcal{M}_{A_L^{\ell,c}:\text{s-channel}} &= \epsilon_{k_1,\mu}\epsilon_{k_2,\nu}\epsilon_{p_1,\alpha}^*\epsilon_{p_2,\beta}^* \\
&\quad (-ig_A f^{abc})^2 \left(g^{\mu\lambda}(2k_1 + k_2)^\nu + g^{\lambda\nu}(-k_1 - 2k_2)^\mu + g^{\nu\mu}(-k_1 + k_2)^\lambda \right) \\
&\quad \frac{1}{s - M_c^2} \left(g^{\lambda\rho} - \frac{1}{M_c^2} (k_1 + k_2)^\lambda (p_1 + p_2)^\rho \right) \\
&\quad \left(g^{\alpha\beta}(p_2 - p_1)^\rho + g^{\beta\rho}(-p_1 - 2p_2)^\alpha + g^{\rho\alpha}(2p_1 + p_2)^\beta \right).
\end{aligned} \tag{3.16}$$

Note that their scalar products will be shown in Appendix C.

$$4. \quad F^i \bar{F}^i \rightarrow A_L^{\ell,a} A_L^{\ell,a}$$

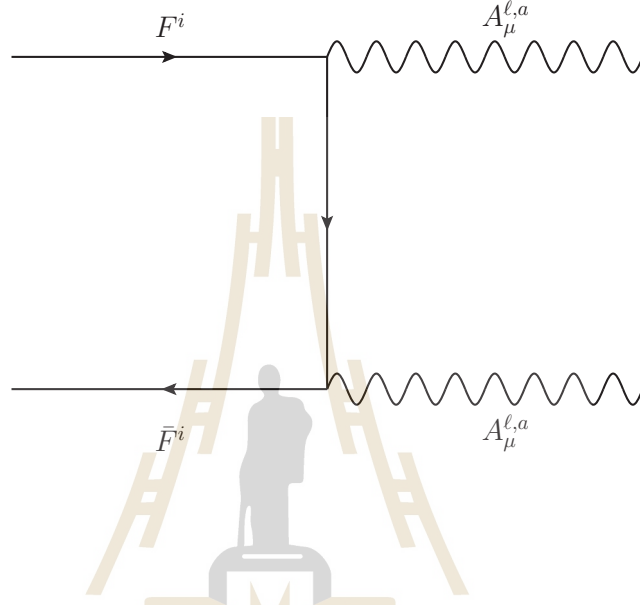
In this process, there are two incoming fermions with flavor i and two outgoing flavor gauge bosons with flavor a . The vertex of gauge boson interaction depends on structure constant, f^{abc} as



$$= g f^{abc} \left(g^{\mu\nu}(k - p)^\rho + g^{\nu\rho}(p - q)^\mu + g^{\rho\mu}(q - k)^\nu \right).$$

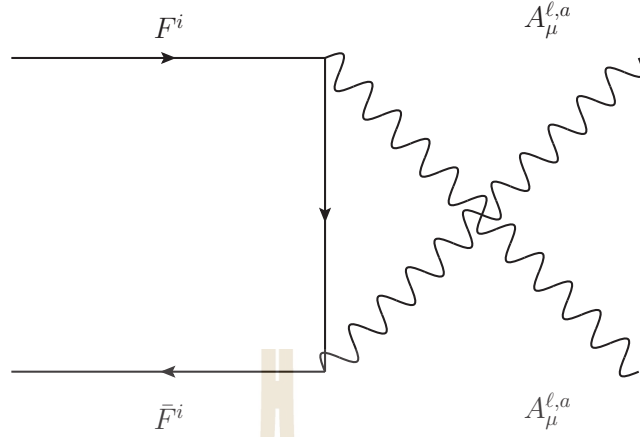
For the s-channel with gauge boson exchange, structure constant is zero as shown in Appendix A. Therefore, it does not have gauge boson exchange in this sector. There are only diagrams in t- and u-channels for fermion exchange.

t-channel:



$$\begin{aligned}
 i\mathcal{M}_{f:t\text{-channel}} &= \bar{v}_2(-ig_\ell\gamma^\mu T^a)\epsilon_4 \frac{-i(\gamma_\mu(p_1 - p_3 + m_i))}{t - m_i} (-ig_\ell\gamma_\nu T^a)\epsilon_3 P_R u_1, \\
 \mathcal{M}_{f:t\text{-channel}} &= \frac{(g_\ell T^a)^2}{t - m_i} \bar{v}_2 \gamma_\mu \epsilon_4 P_R \gamma_\mu (p_1 - p_3 + m_i) \gamma_\nu \epsilon_3 P_R u_1 \\
 &= \frac{(g_\ell T^a)^2 (\sqrt{s - 4m^2} + \sqrt{s})}{8M_A^2 \left((1 - x)(M_A^2 + m_f^2 - s/2) - m_i^2 \right)} \left(\sqrt{s} (-2m_i(\sqrt{s} - x\sqrt{s - 4M_A^2}) \right. \\
 &\quad \left. + i\sqrt{1 - x^2} \sqrt{s - 4m_f^2} (x\sqrt{s} - \sqrt{s - 4M_A^2})) \right. \\
 &\quad \left. + M_A^2 (4m_i - 2i\sqrt{1 - x^2} \sqrt{s - 4M_A^2}) \right). \tag{3.17}
 \end{aligned}$$

u-channel:



$$\begin{aligned}
i\mathcal{M}_{f:\text{u-channel}} &= (-ig_\ell T^a) \bar{v}_2 \gamma^\mu \epsilon_3 \frac{-i(\gamma_\mu(p_1 - p_4 + m_i))}{u - m_i} (-ig_\ell T^a) \gamma_\nu \epsilon_4 P_R u_1, \\
\mathcal{M}_{f:\text{u-channel}} &= \frac{(g_\ell T^a)^2}{u - m_i} \bar{v}_2 \gamma_\mu \epsilon_4 P_R \gamma_\mu (p_1 - p_4 + m_i) \gamma_\nu \epsilon_3 P_R u_1 \\
&= \frac{(g_\ell T^a)^2 (\sqrt{s - 4m^2} + \sqrt{s})}{4M_A^2 \left(-2(x+1)M_A^2 - 2m_f^2(x+1) + 2m_i^2 + sx + s \right)} \left(i\sqrt{s}(\sqrt{1-x^2} \right. \\
&\quad \left. \sqrt{s - 4m_f^2}(\sqrt{s - 4M_A^2} + \sqrt{sx}) + 2im_i(x\sqrt{s - 4M_A^2} + \sqrt{s}) \right. \\
&\quad \left. + M_A^2(4m_i + 2i\sqrt{1-x^2}\sqrt{s - 4M_A^2}) \right). \tag{3.18}
\end{aligned}$$

5. $F^i \bar{F}^j \rightarrow A_L^{\ell,a} A_L^{\ell,b}$

This process is a more general case with a different incoming and outgoing particles. Their 4-momenta and polarization vectors are

$$\begin{aligned}
p_1 &= (E_1, 0, 0, p_i), \\
p_2 &= (E_2, 0, 0, -p_i), \\
p_3 &= (E_3, p_f \sqrt{1-x^2}, 0, p_f x), \\
p_4 &= (E_4, -p_f \sqrt{1-x^2}, 0, -p_f x),
\end{aligned} \tag{3.19}$$

where $E_1^2 = p_i^2 + M_i^2$, $E_2^2 = p_i^2 + M_j^2$, $E_3^2 = p_j^2 + M_a^2$ and $E_4^2 = p_j^2 + M_b^2$. Thus incoming momentum, outgoing momentum and Mandelstam's variables in term of energy are

$$\begin{aligned}
p_i &= \frac{M_i^4 + (M_j^2 - s)^2 - 2M_i^2(M_j^2 + s)}{2\sqrt{s}}, \\
p_f &= \frac{M_a^4 + (M_b^2 - s)^2 - 2M_a^2(M_b^2 + s)}{2\sqrt{s}}, \\
t &= M_a^2 + M_i^2 - 2\sqrt{M_a^2 + \frac{M_a^4 + (M_b^2 - s)^2 - 2m_a^2(M_b^2 + s)}{4s}} \\
&\quad \sqrt{M_i^2 + \frac{M_i^4 + (M_j^2 - s)^2 - 2m_a^2(M_j^2 + s)}{4s}} \\
&\quad + \frac{1}{2s} \sqrt{M_a^4 + (M_b^2 - s)^2 - 2M_a^2(M_b^2 + s)} \sqrt{M_i^4 + (M_j^2 - s)^2 - 2M_i^2(M_j^2 + s)} x, \\
u &= M_b^2 + M_i^2 - 2\sqrt{M_b^2 + \frac{M_a^4 + (M_b^2 - s)^2 - 2m_a^2(M_b^2 + s)}{4s}} \\
&\quad \sqrt{M_i^2 + \frac{M_i^4 + (M_j^2 - s)^2 - 2m_a^2(M_j^2 + s)}{4s}} \\
&\quad - \frac{1}{2s} \sqrt{M_a^4 + (M_b^2 - s)^2 - 2M_a^2(M_b^2 + s)} \sqrt{M_i^4 + (M_j^2 - s)^2 - 2M_i^2(M_j^2 + s)} x.
\end{aligned} \tag{3.20}$$

We will calculate amplitudes in both t-and u-channel following the same products as in $F^i \bar{F}^i \rightarrow A_L^{\ell,a} A_L^{\ell,a}$ amplitudes.

CHAPTER IV

PARTIAL WAVE UNITARITY CONSTRAINT

This chapter discusses the application of partial wave unitarity constraint (PWUC) on our tree level amplitudes. It implies that the sum of all amplitudes cannot grow arbitrarily large with the energy. The idea of unitarity was originated from the assumption that the probability must be conserved. To apply this unitary bound, the scattering amplitude will be decomposed into partial wave eigenbases. The coefficient of each eigenmode must be consistent with the unitary condition.

For the simplest process of this theoretical bound (Schwartz, 2014), consider a $2 \rightarrow 2$ elastic scattering in the center-of-mass frame: $A(p_1) + B(p_2) \rightarrow A(p_3) + B(p_4)$. The total cross-section is

$$\sigma_{total}(AB \rightarrow AB) = \frac{1}{32\pi E_{cm}^2} \int d\cos\theta |\mathcal{M}(\theta)|^2. \quad (4.1)$$

Then, the amplitude can be written in terms of partial waves which are related to Legendre polynomials $P_j(\cos\theta)$,

$$\mathcal{M}(\theta) = 16\pi \sum_{j=0}^{\infty} a_j (2j+1) P_j(\cos\theta). \quad (4.2)$$

By using the orthogonality of Legendre polynomials

$$\int_{-1}^1 P_j(\cos\theta) P_k(\cos\theta) d\cos\theta = \frac{2}{2j+1} \delta_{jk}, \quad (4.3)$$

together with the optical theorem,*

$$\text{Im}\mathcal{M}(AB \rightarrow AB)|_{\theta=0} \geq 2E_{cm}|\vec{p}_i|\sigma_{total}(AB \rightarrow AB), \quad (4.4)$$

one gets

$$\sum_{j=0}^{\infty} (2j+1)\text{Im}(a_j) \geq \frac{2|\vec{p}_i|}{E_{cm}} \sum_{j=0}^{\infty} (2j+1)|a_j|^2. \quad (4.5)$$

This inequality gives an upper bound on each coefficient $|a_j|$. For any complex number z , the magnitude of z should not be less than the imaginary part of z . It gives us $|a_j| \geq \text{Im}(a_j)$ or the lower bound of $|a_j|$. To clearly understand these two conditions, let's assume this scattering in the high energy limit, $E_{cm} \gg m_A, m_B$ or $|\vec{p}| = \frac{1}{2}E_{cm}$. Then we get $\text{Im}(a_j) = |a_j|^2$ and it implies the boundary of $|a_j|$ as shown in Figure 4.1. This can be translated to bounds on component of a_j :

$$|a_j| \leq 1, \quad 0 \leq \text{Im}(a_j) \leq 1 \quad \text{and} \quad |\text{Re}(a_j)| \leq \frac{1}{2}. \quad (4.6)$$

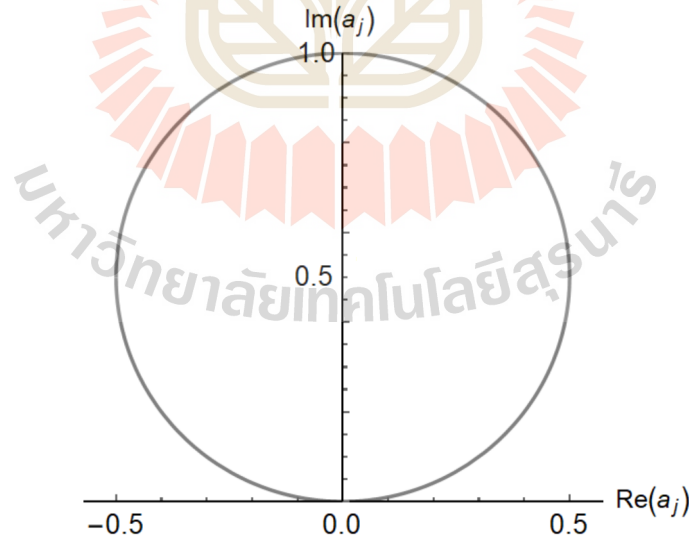


Figure 4.1 Boundary of a_j for $AB \rightarrow AB$ process at high energy limit.

These bounds constrain the behavior of elastic scattering, $AB \rightarrow AB$, in the high energy limit. As an application of partial wave unitarity constraint Lee, Quigg

*This theory showed the relationship between the scattering amplitude and experimental quantities, i.e. cross-section and decay rate, then it can imply that $\text{Im}\mathcal{M} \leq |\mathcal{M}|^2$

and Thacker (LQT) derived the bounds on the Higgs boson mass. There, they considered six different scattering amplitudes involving the electroweak gauge bosons and the Higgs boson such as $W_L^+W_L^- \rightarrow W_L^+W_L^-$, $HZ_L \rightarrow HZ_L$ and $HH \rightarrow W_L^+W_L^-$ (Lee et al., 1977). The amplitudes at high energy were decomposed in partial waves which were then subjected to unitarity. Since the amplitude is proportional to Higgs boson mass, unitarity allows one to extract the upper bound on Higgs boson mass.

The same idea can be applied to BSM models. Generically there will be additional contributions to the gauge boson scattering amplitude and a partial wave unitarity bound will be applied on all amplitudes. First, we evaluate amplitudes at high energy limit. After we sum all diagrams, the part of amplitude which grows with energy will be canceled by gauge invariance and renormalizability of the model. Therefore, only the part of amplitude at order $\mathcal{O}(s^0)$ will be employed in this perturbative bound.

1. $F^i \bar{F}^i \rightarrow F^j \bar{F}^j$

s-channel:

$$\mathcal{M}_{A_\ell^a:s\text{-channel}} = - (g_t T_{ij}^a)^2 \frac{(x+1)(\sqrt{s} + \sqrt{s-4m_f^2})^2}{4(s-M_A^2)}. \quad (4.7)$$

At high energy, $s \rightarrow \infty$,

$$\mathcal{M}_{A_\ell^a:s\text{-channel}}|_{\mathcal{O}(s^0)} = - (g_t T_{ij}^a)^2 (x+1), \quad (4.8)$$

where $x \equiv \cos \theta$.

t-channel:

$$\mathcal{M}_{A_\ell^a:\text{t-channel}} = - (g_l T_{ij}^a)^2 \frac{(x+1)(\sqrt{s} + \sqrt{s-4m_f^2})^2}{4M_A^2 + 2(1-x)(s-4m_f^2)}. \quad (4.9)$$

At high energy, $s \rightarrow \infty$,

$$\mathcal{M}_{A_\ell^a:\text{t-channel}}|_{\mathcal{O}(s^0)} = - (g_l T_{ij}^a)^2 \frac{2(x+1)}{x-1}. \quad (4.10)$$

u-channel:

$$\mathcal{M}_{A_\ell^a:\text{u-channel}} = - (g_l T_{ij}^a)^2 \frac{(x-1)(\sqrt{s} + \sqrt{s-4m_f^2})^2}{4M_A^2 + 2(1+x)(s-4m_f^2)}. \quad (4.11)$$

At high energy, $s \rightarrow \infty$,

$$\mathcal{M}_{A_\ell^a:\text{u-channel}}|_{\mathcal{O}(s^0)} = (g_l T_{ij}^a)^2 \frac{2(x-1)}{x+1}. \quad (4.12)$$

Sum of all channels:

$$\mathcal{M}_{A_\ell^a:\text{sum}}|_{\mathcal{O}(s^0)} = - (g_l T_{ij}^a)^2 \frac{x^3 + x^2 - 9x - 1}{x^2 + 1}. \quad (4.13)$$

To get the bound on flavor gauge boson mass which is inversely proportional to the light lepton mass, this gauge boson mass must be encoded in the amplitude. Unfortunately, this amplitude at high energy does not depend on the mass of flavor gauge boson. So this amplitude cannot give the constraint on the light lepton mass.

2. $A_L^{\ell,a} A_L^{\ell,a} \rightarrow A_L^{\ell,b} A_L^{\ell,b}$

This process is more complex than previous processes because their amplitudes depend on a gauge boson mass, M_c , and we do not have information about how large it can be.

The amplitude in t-channel is

$$\mathcal{M} \sim \frac{1}{t - M_c^2}. \quad (4.14)$$

In high energy limit $s \rightarrow \infty$, there is a problem that $t \approx \frac{s}{2}(1 - \cos\theta)$ has a singularity at forward direction ($\theta \approx 0$).

Since M_c can be arbitrary large, it also leads to a divergence of the amplitude at high energy. To deal with such infinity, we rewrite gauge boson mass as $M_c^2 = \epsilon s$ so that

$$\mathcal{M} \sim \frac{1}{t - \epsilon s}. \quad (4.15)$$

The reason we can assume $M_c^2 \rightarrow \epsilon s$ is that a gauge boson mass should be finite when energy grows up. To regulate the scale of gauge boson mass, ϵ was introduced to cut off an increasing of the energy s . Hence, ϵ should be a small value and dimensionless.

t-channel:

$$\begin{aligned} \mathcal{M}_{\text{ansatz: t-channel}} = & \epsilon_{k_1, \mu} \epsilon_{k_2, \nu} \epsilon_{p_1, \alpha}^* \epsilon_{p_2, \beta}^* \\ & (-i g_A f^{abc})^2 \left(g^{\mu\alpha} (k_1 + p_1)^\lambda + g^{\alpha\lambda} (k_1 - 2p_1)^\mu + g^{\lambda\mu} (p_1 - 2k_1)^\alpha \right) \\ & \left(g^{\lambda\rho} - \frac{1}{M_c^2} (k_1 - p_1)^\lambda (p_2 - k_2)^\rho \right) \\ & \left(g^{\nu\beta} (k_2 + p_2)^\rho + g^{\beta\rho} (k_2 - 2p_2)^\nu + g^{\rho\nu} (p_2 - 2k_2)^\beta \right). \end{aligned} \quad (4.16)$$

u-channel:

$$\begin{aligned}
\mathcal{M}_{\text{ansatz: u-channel}} = & \epsilon_{k_1, \mu} \epsilon_{k_2, \nu} \epsilon_{p_1, \alpha}^* \epsilon_{p_2, \beta}^* \\
& (-i g_A f^{abc})^2 \left(g^{\mu\beta} (k_1 + p_2)^\lambda + g^{\beta\lambda} (k_1 - 2p_2)^\mu + g^{\lambda\mu} (p_2 - 2k_1)^\beta \right) \\
& \left(g^{\lambda\rho} - \frac{1}{M_c^2} (k_1 - p_2)^\lambda (p_1 - k_2)^\rho \right) \\
& \left(g^{\nu\alpha} (k_2 + p_1)^\rho + g^{\alpha\rho} (k_2 - 2p_1)^\nu + g^{\rho\nu} (p_1 - 2k_2)^\alpha \right).
\end{aligned} \tag{4.17}$$

sum of all channels:

$$\mathcal{M}_{\text{sum}} = \frac{\mathcal{M}_{\text{ansatz: t-channel}}}{t - \epsilon s} + \frac{\mathcal{M}_{\text{ansatz: u-channel}}}{u - \epsilon s}. \tag{4.18}$$

Next, Mandelstam's variable t and u can be written in term of gauge boson masses and the center of energy into the amplitude:

$$\begin{aligned}
t = & -\left(\frac{s}{2} - (M_a^2 + M_b^2)\right) + \frac{sx}{2} \sqrt{\left(1 - \frac{4M_a^2}{s}\right) \left(1 - \frac{4M_b^2}{s}\right)}, \\
u = & -\left(\frac{s}{2} - (M_a^2 + M_b^2)\right) - \frac{sx}{2} \sqrt{\left(1 - \frac{4M_a^2}{s}\right) \left(1 - \frac{4M_b^2}{s}\right)}.
\end{aligned} \tag{4.19}$$

The amplitude at high energy, $s \rightarrow \infty$, is

$$\mathcal{M}_{\text{sum}} \sim \mathcal{O}(s^0) + \mathcal{O}(s^1). \tag{4.20}$$

Due to the gauge invariance, the term in $\mathcal{O}(s)$ will be canceled if we exactly sum all possible channels including SM gauge boson channels. Now, consider the order s^0 part of the amplitude

$$\mathcal{M}_{\text{sum}} \sim \mathcal{O}(s^0). \tag{4.21}$$

We apply PWUC on this sum of amplitudes by doing partial integration $x = \cos \theta$

in range $[-1, 1]$. We get

$$\int_{-1}^1 \mathcal{M}_{\text{sum}} dx \sim \mathcal{O}(\log(\epsilon)). \quad (4.22)$$

Obviously, this term makes amplitude diverge when ϵ is small. To handle with infinity part, we subtract this term $\mathcal{O}(\log(\epsilon))$ directly from amplitude,

$$\mathcal{M} = \int_{-1}^1 \mathcal{M}_{\text{sum}} dx - \mathcal{O}(\log(\epsilon)). \quad (4.23)$$

Then we take the limit $\epsilon \rightarrow 0$ to get a physical amplitude. Consequently the amplitude of $A_L^{\ell,a} A_L^{\ell,a} \rightarrow A_L^{\ell,b} A_L^{\ell,b}$ without divergence term is

$$\begin{aligned} \mathcal{M}_{aa \rightarrow bb}^{\text{cut off mass}}|_{\epsilon \rightarrow 0} = & (g_A f^{abc})^2 \frac{M_a^4}{M_b^2 M_c^2} + \frac{M_b^4}{M_a^2 M_c^2} + 10 \frac{M_a^2}{M_b^2} + 2 \frac{M_b^2}{M_a^2} \\ & - \frac{M_a^2}{M_c^2} - 8 \frac{M_a}{M_b} + 8 \frac{M_b}{M_a} - \frac{M_b^2}{M_c^2}. \end{aligned} \quad (4.24)$$

However, there is another way to handle with divergence. Since the forward(backward) direction in t-(u-)channel leads to the divergence of the amplitude at high energy limit. To avoid this singularity, we can cut off the integration boundary near the pole such as integrate over $\cos \theta$ in range $[-1, 1 - \epsilon]$ or $[-1 + \epsilon, 1]$ where ϵ is arbitrary small number. This is briefly explained as follows.

The amplitude in t-channel at high energy limit is

$$\mathcal{M}_{\text{t-channel}} \sim \frac{1}{s(1-x)}, \quad (4.25)$$

where $x \equiv \cos \theta$. We take the integral in range $[-1, 1 - \epsilon]$ to decompose it into partial wave mode,

$$\int_{-1}^{1-\epsilon} \mathcal{M}_{\text{t-channel}} dx \sim \mathcal{O}(\log(\epsilon)). \quad (4.26)$$

Next, we subtract the divergence term out similarly with previous technique,

$$\mathcal{M} = \int_{-1}^{1-\epsilon} \mathcal{M}_{\text{t-channel}} dx - \mathcal{O}(\log(\epsilon)). \quad (4.27)$$

Then, we take the limit $\epsilon \rightarrow 0$ on \mathcal{M} so that we get the amplitude in t-channel without the divergence term. For u-channel, we also handle it with the same method where the cut off boundary is $[-1 + \epsilon, 1]$.

Finally, the amplitude of $A_L^{\ell,a} A_L^{\ell,a} \rightarrow A_L^{\ell,b} A_L^{\ell,b}$ by this cut off boundary technique becomes

$$\begin{aligned} \mathcal{M}_{|aa \rightarrow aa}^{\text{cut off boundary}} = & (g_A f^{abc})^2 \frac{1}{4M_a^3 M_b^2 M_c^2} \left(4M_a^7 - M_a^5 (4M_b^2 + M_c^2 (\log(65536) - 44)) \right. \\ & + 2M_a^4 M_b M_c^2 (\log(16) - 16) - 4M_a^3 (M_b^4 + M_b^2 M_c^2 (2 + \log(16))) - 3M_c^4 \\ & + 8M_a^2 M_b M_c^2 (4M_b^2 + M_c^2 (\log(4) - 4)) + 2M_a (2M_b^6 + 6M_b^4 M_c^2 \\ & + 2M_b^2 M_c^4 (\log(16) - 5) - M_c^6 (\log(256) - 2) \\ & \left. - 4M_b^5 M_c^2 \log(4) + M_b M_c^6 \log(256)) \right). \end{aligned} \quad (4.28)$$

3. $A_L^{\ell,a} A_L^{\ell,b} \rightarrow A_L^{\ell,a} A_L^{\ell,b}$

This amplitude is a more general case where the incoming(outgoing) gauge bosons are in different flavors. However, the divergence from forward(backward) direction still appear in this process. To handle with the singularity, we also apply the cut off boundary technique in both s- and t-channel.

The amplitude of $A_L^{\ell,a} A_L^{\ell,b} \rightarrow A_L^{\ell,a} A_L^{\ell,b}$ is

$$\begin{aligned}
\mathcal{M}_{ab \rightarrow ab}^{\text{cut off boundary}} = & (g_A f^{abc})^2 \frac{1}{48M_a^2 M_b^3 M_c^2} \left(48M_a^6 M_b + 84M_a^5 M_c^2 \right. \\
& - 2M_a^4 M_b (24M_b^2 - 122M_c^2) + 24M_a^3 M_b^2 M_c^2 \\
& + 4M_a^2 M_b (-12M_b^4 + M_b^2 M_c^2 (52 - 4 \log(4096))) \\
& + 3M_c^4 (\log(256) - 12)) \\
& - 3M_a M_c^2 (36M_b^4 + 4M_b^2 M_c^2 (\log(16) - 8) + 4M_c^4 \log(4)) \\
& + M_b (48M_b^6 - 68M_b^4 M_c^2 + 6M_b^2 M_c^4 (\log(256) - 12) \\
& \left. - 3M_c^6 (4 \log(64) - 20)) \right). \tag{4.29}
\end{aligned}$$

4. $F^i \bar{F}^i \rightarrow A_L^{l,a} A_L^{l,a}$

t-channel:

At high energy ($s \rightarrow \infty$):

$$\begin{aligned}
\mathcal{M}_{f:\text{t-channel}} = & \frac{(g_\ell T_{ij}^a)^2}{2M_a^2(x+1)} \left(-2m_k x(x+1)\sqrt{s} + 2m_k^2 \sqrt{1-x^2}, \right. \\
& \left. + (2M_a^2 - M_i^2 + s)(x-1)\sqrt{1-x^2} \right)
\end{aligned}$$

$$\mathcal{M}_{f:\text{t-channel}}|_{\mathcal{O}(s^0)} = \frac{(g_\ell T_{ij}^a)^2}{2M_a^2(x+1)} \left(2m_k^2 \sqrt{1-x^2} + (2M_a^2 - M_i^2)(x-1)\sqrt{1-x^2} \right). \tag{4.30}$$

u-channel:

At high energy ($s \rightarrow \infty$):

$$\begin{aligned}\mathcal{M}_{f:\text{u-channel}} &= \frac{(g_\ell T_{ij}^a)^2}{2M_a^2(x+1)} \left(2m_k x(x+1)\sqrt{s} + 2m_k^2\sqrt{1-x^2}, \right. \\ &\quad \left. -(2M_a^2 - M_i^2 + s)(1+x)\sqrt{1-x^2} \right) \\ \mathcal{M}_{f:\text{u-channel}}|_{\mathcal{O}(s^0)} &= \frac{(g_\ell T_{ij}^a)^2}{2M_a^2(x+1)} \left(2m_k^2\sqrt{1-x^2} - (2M_a^2 - M_i^2)(1+x)\sqrt{1-x^2} \right).\end{aligned}\tag{4.31}$$

Sum of all channels:

$$\mathcal{M}_{f:\text{sum}}|_{\mathcal{O}(s^0)} = (g_\ell T_{ij}^a)^2 \frac{m_k^2 x}{M_a^2 \sqrt{1-x^2}}.\tag{4.32}$$

Next, we decompose this amplitude into a partial wave mode by taking a partial integration in range $[-1, 1]$ following the method of PWUC. We obtain

$$\int_{-1}^1 \mathcal{M}_{f:\text{sum}}|_{\mathcal{O}(s^0)} x dx = (g_\ell T_{ij}^a)^2 \frac{m_k^2 \pi}{M_A^2}.\tag{4.33}$$

5. $F^i \bar{F}^j \rightarrow A_L^{l,a} A_L^{l,b}$

t-channel:

At high energy ($s \rightarrow \infty$):

$$\begin{aligned}\mathcal{M}_{f:\text{t-channel}} &= \frac{(g_\ell)^2 T_{ik}^a T_{kj}^b}{4M_a M_b (x-1)} \left(4m_k x \sqrt{s} + 4m_k \sqrt{1-x^2} \right. \\ &\quad \left. + (2M_a^2 + 2M_b^2 - M_i^2 - M_j^2 + 2s)(x-1)\sqrt{1-x^2} \right), \\ \mathcal{M}_{f:\text{t-channel}}|_{\mathcal{O}(s^0)} &= \frac{(g_\ell)^2 T_{ik}^a T_{kj}^b \sqrt{1-x^2}}{4M_a M_b (x-1)} \left(M_i^2 + M_j^2 + 4m_k^2 \right. \\ &\quad \left. + (x-1)(2M_a^2 + 2M_b^2) - x(M_i^2 + M_j^2) \right).\end{aligned}\tag{4.34}$$

u-channel:

At high energy ($s \rightarrow \infty$):

$$\begin{aligned} \mathcal{M}_{f:\text{u-channel}} &= \frac{(g\ell)^2 T_{ik}^a T_{kj}^b}{4M_a M_b (x-1)} \left(4m_k x \sqrt{s} + 4m_k \sqrt{1-x^2} \right. \\ &\quad \left. - (2M_a^2 + 2M_b^2 - M_i^2 - M_j^2 + 2s)(x+1)\sqrt{1-x^2} \right), \\ \mathcal{M}_{f:\text{u-channel}}|_{\mathcal{O}(s^0)} &= \frac{(g\ell)^2 T_{ik}^a T_{kj}^b \sqrt{1-x^2}}{4M_a M_b (x+1)} \left(4m_k^2 \right. \\ &\quad \left. - (2M_a^2 + 2M_b^2 - M_i^2 - M_j^2) \right). \end{aligned} \quad (4.35)$$

Sum of all channels:

$$\mathcal{M}_{f:\text{sum}}|_{\mathcal{O}(s^0)} = (g\ell)^2 T_{ik}^a T_{kj}^b \frac{2m_k^2 x}{M_a M_b \sqrt{1-x^2}}. \quad (4.36)$$

Again, We decompose this amplitude into a partial wave mode by taking a partial integration in range $[-1, 1]$ following the method of PWUC and obtain

$$\int_{-1}^1 \mathcal{M}_{f:\text{sum}}|_{\mathcal{O}(s^0)} x dx = (g\ell)^2 T_{ik}^a T_{kj}^b \frac{m_k^2 \pi}{M_a M_b}. \quad (4.37)$$

Finally, these two processes of fermion exchange can be used to constrain neutrino mass.

Unitarity bound

After amplitudes are decomposed into partial wave mode, they must satisfy unitary bound as described earlier. The general amplitude can be written in partial wave mode as

$$\mathcal{M}(\theta) = 16\pi \sum_{j=0}^{\infty} a_j (2j+1) P_j(\cos \theta). \quad (4.38)$$

For simplicity, mode $j = 0$ is selected,

$$\mathcal{M}(\theta) = 16\pi a_0 P_0(\cos \theta), \quad (4.39)$$

where $P_0(x) = 1$, and

$$a_0 = \frac{1}{16\pi} \int_{-1}^1 \frac{\mathcal{M}}{2} dx. \quad (4.40)$$

After implementing partial wave unitarity constraint, $|\text{Re}(a_j)| \leq \frac{1}{2}$, we got

$$\frac{1}{16\pi} M_0 \leq \frac{1}{2}, \quad (4.41)$$

$$\text{or } M_0 \leq 8\pi,$$

where $2M_0 = \int_{-1}^1 \mathcal{M} dx$ is real. Therefore the amplitudes in partial wave mode with perturbative constraint satisfy

$$\begin{aligned} \mathcal{M}_{aa \rightarrow bb}^{\text{cut off mass}} &\leq 8\pi, \\ \mathcal{M}_{aa \rightarrow bb}^{\text{cut off boundary}} &\leq 8\pi, \\ \mathcal{M}_{ab \rightarrow ab}^{\text{cut off boundary}} &\leq 8\pi. \end{aligned} \quad (4.42)$$

Nevertheless, the amplitudes for $F^i \bar{F}^i \rightarrow A_L^{l,a} A_L^{l,a}$ and $F^i \bar{F}^j \rightarrow A_L^{l,a} A_L^{l,b}$ can be decomposed in $j = 1$ mode of partial wave,

$$16\pi(2a_1) = \int_{-1}^1 \mathcal{M}(\theta) \cos \theta d(\cos \theta), \quad (4.43)$$

$$a_1 = \frac{M_1}{16\pi}$$

where $P_1(x) = x$ and $2M_1 = \int_{-1}^1 \mathcal{M}(\theta) \cos \theta d(\cos \theta)$ is real. They also satisfy $|\text{Re}(a_j)| \leq \frac{1}{2}$, so we got

$$(g_\ell T_{ij}^a)^2 \frac{m_k^2 \pi}{2M_a^2} \leq 8\pi, \quad (4.44)$$

and

$$(g_\ell)^2 T_{ik}^a T_{kj}^b \frac{m_k^2 \pi}{2M_a M_b} \leq 8\pi. \quad (4.45)$$

Finally, we obtained the bounds on amplitude in partial wave mode in each process. Next chapter, we will combine these theoretical constraints with

experimental data to constrain a lower bound on neutrino spectrum.



CHAPTER V

NEUTRINO SPECTRUM

In this chapter we employ a choice of basis where $\langle \mathcal{Y}_N \rangle$ is diagonal. We use the convention $m_{\mu_1} < m_{\mu_2} < m_{\mu_3}$ for the ordering of neutrino masses in this work for both the normal and the inverted hierarchy. In order to obtain a lower bound on the lightest neutrino mass, we have to know what constraints on neutrino masses in recent experiments are. Then we will combine constraints from neutrino data and theoretical constraint which we had calculated in the previous chapter. Finally, we will present a plot of the ratio of neutrino masses and translate it to the lower bound on the lightest neutrino mass. Moreover, we can reverse our result to determine other SM neutrino masses.

First, we list the latest neutrino information from experiments in table 5.1. We want to emphasize that this work uses a special convention for the ordering of neutrino mass. For instance, m_{ν_1} (m_{ν_3}) was labeled to be the lightest (heaviest) neutrino mass in both normal and inverted hierarchy. This is in contrast with a global convention, where m_{ν_1} is the lightest neutrino mass in the normal hierarchy and m_{ν_3} is the lightest for the inverted hierarchy as shown in figure 5.1.

Table 5.1 Current neutrino data from neutrino oscillation.

Parameter	best-fit	3σ
$m_{\nu_3}^2 - m_{\nu_1}^2$ (NH) [10^{-3} eV]	2.56	2.45-2.69
$m_{\nu_2}^2 - m_{\nu_1}^2$ (NH) [10^{-5} eV]	7.37	6.93-7.96
$m_{\nu_3}^2 - m_{\nu_1}^2$ (IH) [10^{-3} eV]	2.54	2.42-2.66
$m_{\nu_3}^2 - m_{\nu_2}^2$ (IH) [10^{-5} eV]	7.37	6.93-7.96

In addition, there are constraints from the cosmic microwave background

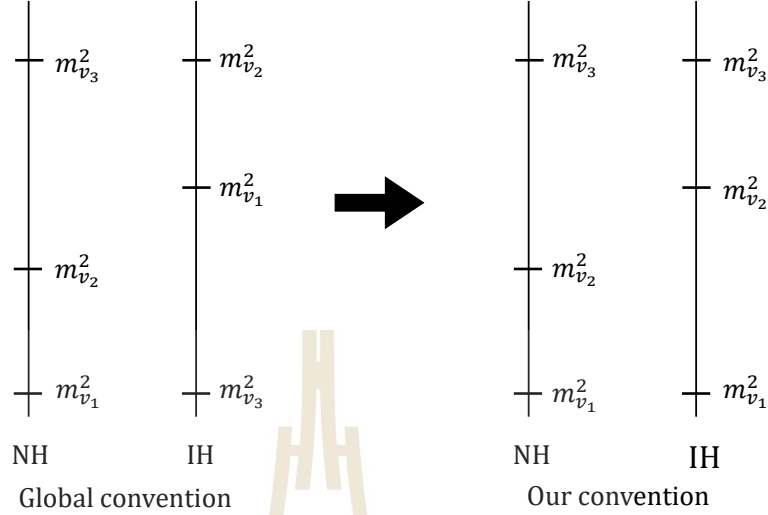


Figure 5.1 Comparison between global convention and this work convention and baryonic acoustic oscillation (Tanabashi et al., 2018),

$$\sum m_{\nu_i} \leq 0.17 \text{ eV} \quad 95\% \text{CL..} \quad (5.1)$$

This equation (5.1) explains that the sum of all light neutrino masses is lower than 0.17 eV. Obviously, these information show that only experimental data cannot determine the lower bound of the lightest neutrino mass, m_{ν_1} . In order to complete this bound, we have to combine it with theoretical constraint from previous chapter.

Since the amplitude in equation (4.42) depends on the flavor gauge group structure constant, we have to calculate all possible flavor interactions and then examine the most effective process on neutrino mass and mixing bound. The number of total calculated amplitudes is $8 \times 8 = 64$.

For the result, the process $A_L^{\ell,a} A_L^{\ell,a} \rightarrow A_L^{\ell,b} A_L^{\ell,b}$ and $A_L^{\ell,a} A_L^{\ell,b} \rightarrow A_L^{\ell,a} A_L^{\ell,b}$ involve divergence in the forward direction. Since there is an ambiguity in how the singularity is removed (see (4.24) and (4.28)), we will not use them in our

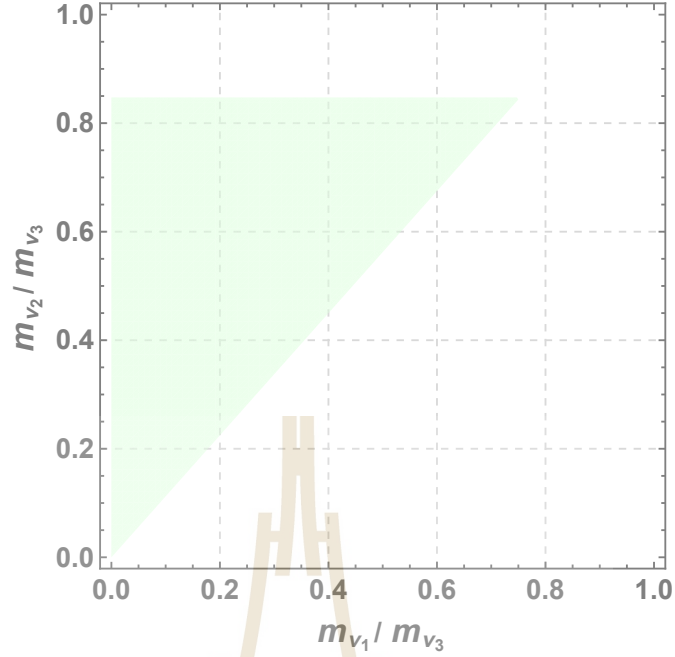


Figure 5.2 The region of perturbative unitary bound on neutrino spectrum when $\langle \mathcal{Y}_N \rangle$ is diagonal.

numerical analysis.

The processes $F^i \bar{F}^i \rightarrow A_L^{l,a} A_L^{l,a}$ and $F^i \bar{F}^j \rightarrow A_L^{l,a} A_L^{l,b}$ give us the constraint on neutrino masses as shown in figure 5.2. In order to investigate the lowest bound on the lightest neutrino, we follow these steps:

1. Pick up values of neutrino mass from current neutrino data in table 5.1 and equation (5.1).

For the normal hierarchy $m_{\nu_1} \lesssim m_{\nu_2} \ll m_{\nu_3}$, the range of the selected values are

$$\begin{aligned}
 m_{\nu_3}^2 - m_{\nu_1}^2 &\in [2.45, 2.69] \times 10^{-3}, \\
 m_{\nu_3}^2 \left(1 - \frac{m_{\nu_1}^2}{m_{\nu_3}^2}\right) &\in [2.45, 2.69] \times 10^{-3}, \\
 \frac{m_{\nu_1}^2}{m_{\nu_3}^2} &\in \left[1 - \frac{2.69 \times 10^{-3}}{m_{\nu_3}^2}, 1 - \frac{2.45 \times 10^{-3}}{m_{\nu_3}^2}\right],
 \end{aligned} \tag{5.2}$$

and

$$m_{\nu_2}^2 - m_{\nu_1}^2 \in [6.93, 7.96] \times 10^{-5},$$

$$m_{\nu_3}^2 \left(\frac{m_{\nu_2}^2}{m_{\nu_3}^2} - \frac{m_{\nu_1}^2}{m_{\nu_3}^2} \right) \in [6.93, 7.96] \times 10^{-5}, \quad (5.3)$$

$$\frac{m_{\nu_2}^2}{m_{\nu_3}^2} \in \left[\frac{m_{\nu_1}^2}{m_{\nu_3}^2} + \frac{6.93 \times 10^{-5}}{m_{\nu_3}^2}, \frac{m_{\nu_1}^2}{m_{\nu_3}^2} + \frac{7.96 \times 10^{-5}}{m_{\nu_3}^2} \right],$$

where $m_{\nu_3} \in [\sqrt{2.69 \times 10^{-3}}, 0.17]$.

For the inverted hierarchy $m_{\nu_1} \ll m_{\nu_2} \lesssim m_{\nu_3}$, the range of the selected values are

$$m_{\nu_3}^2 - m_{\nu_1}^2 \in [2.42, 2.66] \times 10^{-3},$$

$$m_{\nu_3}^2 \left(1 - \frac{m_{\nu_1}^2}{m_{\nu_3}^2} \right) \in [2.42, 2.66] \times 10^{-3}, \quad (5.4)$$

$$\frac{m_{\nu_1}^2}{m_{\nu_3}^2} \in \left[1 - \frac{2.66 \times 10^{-3}}{m_{\nu_3}^2}, 1 - \frac{2.42 \times 10^{-3}}{m_{\nu_3}^2} \right],$$

$$m_{\nu_3}^2 - m_{\nu_2}^2 \in [6.93, 7.96] \times 10^{-5},$$

$$m_{\nu_3}^2 \left(1 - \frac{m_{\nu_2}^2}{m_{\nu_3}^2} \right) \in [6.93, 7.96] \times 10^{-5}, \quad (5.5)$$

$$\frac{m_{\nu_2}^2}{m_{\nu_3}^2} \in \left[1 - \frac{7.96 \times 10^{-5}}{m_{\nu_3}^2}, 1 - \frac{6.93 \times 10^{-5}}{m_{\nu_3}^2} \right],$$

where $m_{\nu_3} \in [\sqrt{2.66 \times 10^{-3}}, 0.17]$.

2. Scan of values of neutrino masses under cosmological and partial wave unitarity constraint

$$m_{\nu_3} \left(\frac{m_{\nu_1}}{m_{\nu_3}} + \frac{m_{\nu_2}}{m_{\nu_3}} + 1 \right) \leq 0.17 \quad \text{eV}, \quad (5.6)$$

and

$$\mathcal{M} \leq 8\pi. \quad (5.7)$$

By following above steps, the result of neutrino spectra in both hierarchies is shown in figure 5.3

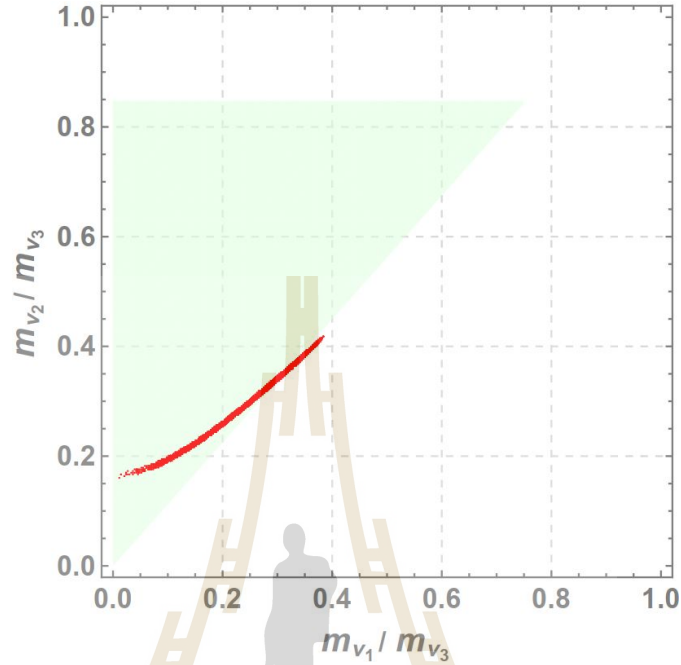


Figure 5.3 Viable neutrino spectra for normal hierarchy (red). Region compatible with perturbative unitarity is shown in green.

Notice that there is no viable neutrino spectra for inverted hierarchy in figure 5.3. The reason is that the perturbative unitarity region is not large enough to accommodate the inverted hierarchy mass ratio. Therefore there is only the red region for normal hierarchy.

Since values of neutrino spectra in figure 5.3 are given in terms of the ratio between two different light neutrino mass, to evaluate the lower bound of the lightest neutrino mass m_{ν_1} , we will multiply it by m_{ν_3} . Thus, the result of lower bound on neutrino spectrum is $m_{\nu_1} \geq 6.11 \times 10^{-4}$ eV for the normal hierarchy.

From the lower bound on m_{ν_1} , we can deduce the lower bound on the other two neutrino masses by using neutrino mass squared differences from table 5.1, as shown in figure 5.4. Figure 5.4 shows how does the lightest neutrino mass is related to the other neutrino masses. If a lower bound on the lightest neutrino

mass m_{ν_1} is identified, the lower bounds on m_{ν_2} and m_{ν_3} will be determined.

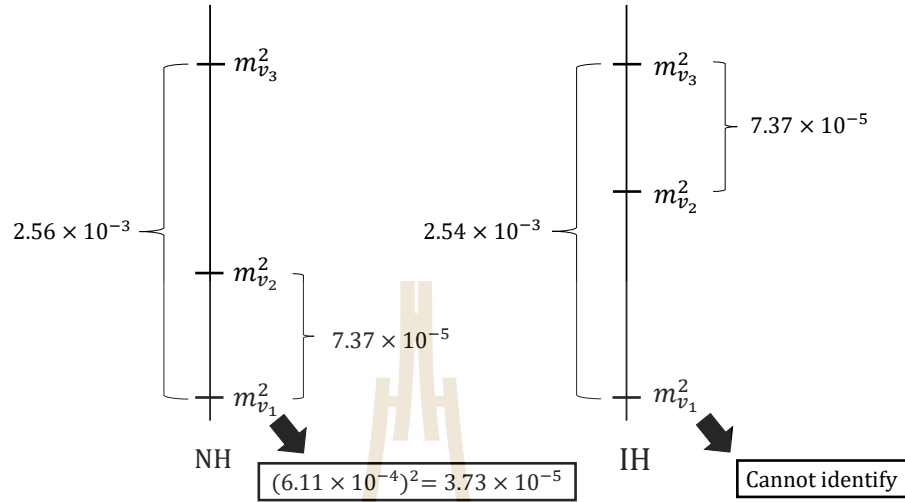


Figure 5.4 Scale of neutrino mass squared differences in normal and inverted hierarchy.

However, notice that the bound on neutrino mass comes from a $\langle \mathcal{Y}_N \rangle$ diagonal basis choice. There is also a choice of diagonal $\langle \mathcal{Y}_E \rangle$. We will next work in this basis where neutrino mixing is apparent. In the next chapter, we will go back to our Lagrangian and indicate how lepton mixing matrix appear in an interaction. Then we will employ a PWUC to constrain neutrino mixing angles.

CHAPTER VI

NEUTRINO MIXING

In this chapter we discuss how to obtain a conservative bound of neutrino mixing parameter. Since $\langle \mathcal{Y}_E \rangle$ and $\langle \mathcal{Y}_N \rangle$ can not be diagonalized simultaneously, lepton mixing angles are only encoded in $\langle \mathcal{Y}_N \rangle$ when we choose basis of diagonal $\langle \mathcal{Y}_E \rangle$. Thus, a suitable basis choice for studying neutrino mixing constraint is the one where $\langle \mathcal{Y}_E \rangle$ is diagonal.

In order to study mixing parameter, the relevant interactions in the Lagrangian are the Yukawa interactions. For this gauged lepton flavor model, it has three extra fermions. Their Yukawa interactions are

$$\mathcal{L}_{\text{Yuk}} = \lambda_E \bar{\ell}_L H \mathcal{E}_R + \mu_E \bar{\mathcal{E}}_L e_R + \lambda_\varepsilon \bar{\mathcal{E}}_L \mathcal{Y}_E \mathcal{E}_R + \lambda_\nu \bar{\ell}_L \tilde{H} \mathcal{N}_R + \frac{\lambda_N}{2} \bar{\mathcal{N}}_R^c \mathcal{Y}_N \mathcal{N}_R + \text{h.c.}, \quad (6.1)$$

where $\tilde{H} \equiv i\sigma_2 H^*$ with hypercharge $-1/2$. After both electroweak and flavor symmetries are broken spontaneously by background of the scalars

$$H \equiv \frac{1}{\sqrt{2}} \begin{pmatrix} 0 \\ v + h \end{pmatrix}, \quad (6.2)$$

$$\mathcal{Y}_E \equiv \langle \mathcal{Y}_E \rangle + \phi_E / \sqrt{2},$$

$$\mathcal{Y}_N \equiv \langle \mathcal{Y}_N \rangle + \phi_N / \sqrt{2},$$

the Yukawa interaction becomes

$$\begin{aligned}
\mathcal{L}_{\text{Yuk}} = & \lambda_E \begin{pmatrix} \nu_L & e_L \end{pmatrix} \frac{1}{\sqrt{2}} \begin{pmatrix} 0 \\ v+h \end{pmatrix} \mathcal{E}_R + \mu_E \overline{\mathcal{E}}_L e_R + \lambda_E \overline{\mathcal{E}}_L \langle \mathcal{Y}_E \rangle \mathcal{E}_R \\
& + \lambda_\nu \frac{1}{\sqrt{2}} \begin{pmatrix} \nu_L & e_L \end{pmatrix} i\sigma_2 \begin{pmatrix} 0 \\ v+h \end{pmatrix} \mathcal{N}_R + \frac{\lambda_N}{2} \overline{\mathcal{N}}_R^c \langle \mathcal{Y}_N \rangle \mathcal{N}_R + \text{h.c.},
\end{aligned} \tag{6.3}$$

$$\mathcal{L}_{\text{Yuk}} \supset \frac{\lambda_E v}{\sqrt{2}} \overline{e}_L \mathcal{E}_R + \mu_E \overline{\mathcal{E}}_L e_R + \lambda_E \overline{\mathcal{E}}_L \langle \mathcal{Y}_E \rangle \mathcal{E}_R + \frac{\lambda_\nu v}{\sqrt{2}} \overline{\nu}_L \mathcal{N}_R + \frac{\lambda_N}{2} \overline{\mathcal{N}}_R^c \langle \mathcal{Y}_N \rangle \mathcal{N}_R + \text{h.c.} \tag{6.4}$$

The lepton masses can be written as in (2.13). Assuming $\langle \mathcal{Y}_E \rangle \gg v, \mu_E$ and $\langle \mathcal{Y}_N \rangle \gg v$, the Lagrangian of the light lepton mass is given by

$$\mathcal{L}_{\text{light mass}} \supset \overline{e}_L m_l e_R + \nu_L m_\nu \nu_L, \tag{6.5}$$

where $m_l(m_\nu)$ is a light electron(neutrino) mass.

Since e_L and ν_L are in electroweak doublets, they transform equivalently under the orthogonal matrix. To obtain a diagonalized mass matrix, an orthogonal matrix is selected to rotate the flavor basis. In case that light electron mass is diagonalized by V_L^e , the electroweak doublet transform as

$$\begin{aligned}
\ell_L &= \begin{pmatrix} \nu_L \\ e_L \end{pmatrix}, \\
V_L^e \ell_L &= \begin{pmatrix} V_L^e \nu_L \\ V_L^e e_L \end{pmatrix} = \begin{pmatrix} V_L^e (V_L^{\nu\dagger} V_L^\nu) \nu_L \\ V_L^e e_L \end{pmatrix} = \begin{pmatrix} V_L^e V_L^{\nu\dagger} \hat{\nu}_L \\ \hat{e}_L \end{pmatrix} = \begin{pmatrix} U_{\text{PMNS}} \hat{\nu}_L \\ \hat{e}_L \end{pmatrix},
\end{aligned} \tag{6.6}$$

where $U_{\text{PMNS}} \equiv V_L^e V_L^{\nu\dagger}$ is the Pontecorvo-Maki-Nakagawa-Sakata (PMNS) matrix.

This matrix contains the 3 angle parameters: θ_{12} , θ_{23} and θ_{13} , together with a CP-

violating phase or Dirac phase and two Majorana phases: δ , α_{21} and α_{31} . The PMNS matrix can be written as

$$U_{\text{PMNS}} = \begin{pmatrix} c_{12}c_{13} & s_{12}c_{13} & s_{13}e^{-i\delta} \\ -s_{12}c_{23} - c_{12}s_{23}s_{13}e^{i\delta} & c_{12}c_{23} - s_{12}s_{23}s_{13}e^{i\delta} & s_{23}c_{13} \\ s_{12}s_{23} - c_{12}c_{23}s_{13}e^{i\delta} & -c_{12}s_{23} - s_{12}c_{23}s_{13}e^{i\delta} & c_{23}c_{13} \end{pmatrix} \text{diag}(1, e^{i\frac{\alpha_{21}}{2}}, e^{i\frac{\alpha_{31}}{2}}) \quad (6.7)$$

where $s_{ij} \equiv \sin \theta_{ij}$, $c_{ij} \equiv \cos \theta_{ij}$ and U_{PMNS} is the unitary matrix which satisfies $U_{\text{PMNS}}^\dagger U_{\text{PMNS}} = 1$.

The Lagrangian of light lepton mass after light charged lepton mass was diagonalized is

$$\mathcal{L}_{\text{light mass}} \supset \hat{e}_L \hat{m}_l \hat{e}_R + \hat{\nu}_L U_{\text{PMNS}}^\dagger \hat{m}_\nu U_{\text{PMNS}} \hat{\nu}_L, \quad (6.8)$$

where $\hat{m}_l = V_L^e m_{e_L} V_L^{e\dagger}$ ($\hat{m}_\nu = V_L^\nu m_{\nu_L} V_L^{\nu\dagger}$) is the diagonal light electron(neutrino) mass and the mass eigenstate transforms as

$$\hat{e}_L = V_L^e e_L, \quad (6.9)$$

$$\hat{\nu}_L = V_L^\nu \nu_L,$$

where V_L^e (V_L^ν) is an orthogonal matrix for rotating the flavor basis e_L (ν_L) to the mass basis \hat{e}_L ($\hat{\nu}_L$).

For simplicity, we ignore effect from CP-violating phase and Majorana phases. Since the heavy lepton mass is inversely proportional to the light lepton mass in the gauged lepton flavor model such as $M_N \sim m_\nu^{-1} \sim \langle \mathcal{Y} \rangle$. The other basis choice is

$$\langle \hat{\mathcal{Y}}_E \rangle \simeq \frac{\lambda_E \mu_E}{\sqrt{2} \lambda_\mathcal{E}} \text{diag} \left(\frac{v}{m_e}, \frac{v}{m_\mu}, \frac{v}{m_\tau} \right), \quad (6.10)$$

and

$$\langle \hat{\mathcal{Y}}_N \rangle \simeq \frac{\lambda_\nu^2 v}{2\lambda_N} U_{PMNS}^* \text{diag} \left(\frac{v}{m_{\nu_1}}, \frac{v}{m_{\nu_2}}, \frac{v}{m_{\nu_3}} \right) U_{PMNS}^\dagger. \quad (6.11)$$

This basis choice leads to the encoding of the mixing parameters in the gauge boson mass

$$(M_{\ell\ell}^2)_{ab} \simeq g_\ell^2 \left[\text{Tr} \left(\hat{\mathcal{Y}}_N \{T^a, T^b\} \hat{\mathcal{Y}}_N^\dagger \right) + \text{Tr} \left(\mathcal{Y}_N^\dagger \{T^{aT}, T^{bT}\} \mathcal{Y}_N \right) \right. \\ \left. + 2 \text{Tr} \left(\mathcal{Y}_N^\dagger T^{aT} \hat{\mathcal{Y}}_N T^b + \mathcal{Y}_N^\dagger T^{bT} \hat{\mathcal{Y}}_N T^a \right) \right]. \quad (6.12)$$

In previous chapter, the gauge boson mass matrix appears in scattering amplitudes. Thus, these mixing parameters can also be encoded in amplitudes.

1. Constraint on neutrino mixing parameter

In order to constrain neutrino mixing parameters which are encoded in U_{PMNS} , we ignore the Dirac phase and Majorana phase for simplicity. Only $\sin \theta_{23}$, $\sin \theta_{12}$ and $\sin \theta_{13}$ are studied in this work. By varying these three mixing angles, $\sin \theta_{23}$ is the most sensitive parameter with unitary constraint. It is not so surprising because $\sin \theta_{23}$ is the largest value in table 6.1 compared with another two angles. Therefore, we fix $\sin \theta_{12}$ and $\sin \theta_{13}$ then scan the $\sin \theta_{23}$ for both normal and inverted hierarchies.

Figure 6.1 shows grid chart of scanning mixing parameter $\sin \theta_{23}$ at each order pair of $(\sin \theta_{13}, \sin \theta_{12})$. Red dots are a position of scanned $\sin \theta_{23}$. Arrows show how we step the value of $\sin \theta_{12}$ and $\sin \theta_{13}$ in range 3σ .

In figure 6.2, blue region was constrained in the mixing parameter scan. Unfortunately, it cannot constrain $\sin \theta_{23}$ in normal hierarchy because all viable neutrino spectrum is in perturbative region. It means that the effect of neutrino mixing parameter does not give additional constraint from our perturbative region

Table 6.1 The best-fit($\pm 1\sigma$) of three neutrino oscillation from the present experiment neutrino data(Patrignani et al., 2016) and $\sin \theta_{23}$ [NH/IH] from propagating errors (Tanabashi et al., 2018).

Parameter	best-fit($\pm 1\sigma$)
$\Delta m_{21}^2 [10^{-5} eV^2]$	7.37 ± 0.17
$\Delta m_{31(23)}^2 [10^{-3} eV^2]$	$2.56 \pm 0.04 (2.54 \pm 0.04)$
$\sin^2 \theta_{12}$ [NH/IH]	0.297 ± 0.017
$\sin^2 \theta_{23}$ [NH]	0.425 ± 0.039
$\sin^2 \theta_{13}$ [NH]	0.0215 ± 0.0025
$\sin^2 \theta_{23}$ [IH]	0.589 ± 0.042
$\sin^2 \theta_{13}$ [IH]	0.0216 ± 0.0026
$\sin \theta_{23}$ [NH]	0.652 ± 0.030
$\sin \theta_{23}$ [IH]	0.768 ± 0.027

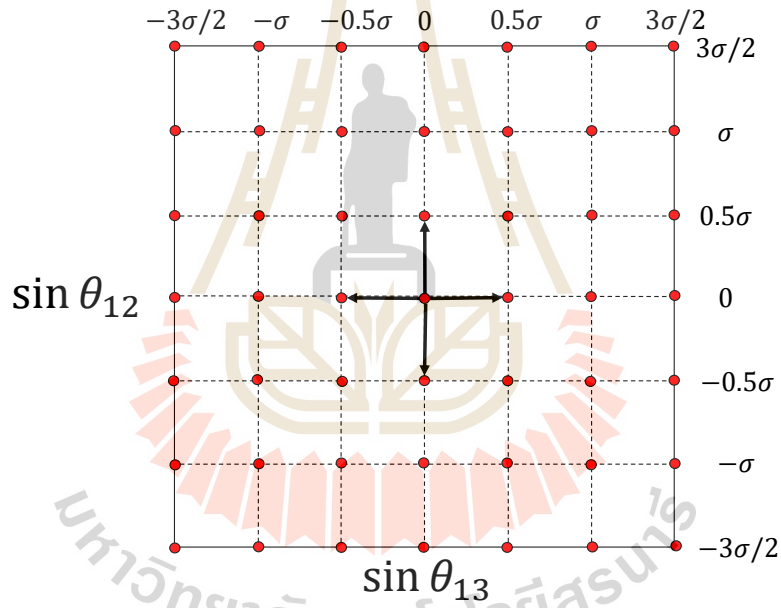


Figure 6.1 Grid chart for scanning mixing parameter when red dots stand for $(\sin \theta_{23})_{ij}$ at $(\sin \theta_{13})_i, (\sin \theta_{12})_j$.

in both hierarchies.

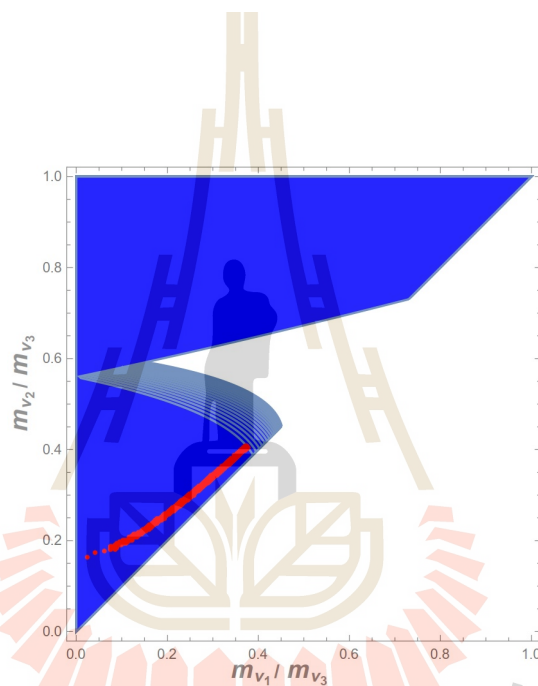


Figure 6.2 Result from scanning mixing parameters in range 2σ . Blue region is the perturbative region. Red line is viable neutrino spectrum for normal hierarchy.

CHAPTER VII

CONCLUSION AND DISCUSSIONS

In this work, we study constraints on neutrino masses and mixings in the $SU(3)_\ell \times SU(3)_E$ model. We use two different bases for the flavon vev. In order to bound neutrino masses, we choose the basis where $\langle \mathcal{Y}_N \rangle$ is diagonal. To constrain neutrino mixing, on the other hand, we choose the basis where $\langle \mathcal{Y}_E \rangle$ is diagonal. First we found that this gauged lepton flavor model gives us the relationship between flavor gauge bosons masses and the light neutrino masses. To connect it with the partial wave unitarity constraint, we have to compute 2-2 scattering amplitudes at tree-level of five processes: $F^i \bar{F}^i \rightarrow F^j \bar{F}^j$, $A_L^{\ell,a} A_L^{\ell,a} \rightarrow A_L^{\ell,b} A_L^{\ell,b}$, $A_L^{\ell,a} A_L^{\ell,b} \rightarrow A_L^{\ell,a} A_L^{\ell,b}$, $F^i \bar{F}^i \rightarrow A_L^{\ell,a} A_L^{\ell,a}$ and $F^i \bar{F}^j \rightarrow A_L^{\ell,a} A_L^{\ell,b}$.

Unfortunately, processes $F^i \bar{F}^i \rightarrow F^j \bar{F}^j$, $A_L^{\ell,a} A_L^{\ell,a} \rightarrow A_L^{\ell,b} A_L^{\ell,b}$ and $A_L^{\ell,a} A_L^{\ell,b} \rightarrow A_L^{\ell,a} A_L^{\ell,b}$ cannot give us a meaningful constraint. Only these two processes: $F^i \bar{F}^i \rightarrow A_L^{\ell,a} A_L^{\ell,a}$ and $F^i \bar{F}^j \rightarrow A_L^{\ell,a} A_L^{\ell,b}$, give us the perturbative unitary constraints. By imposing unitarity constraint, we identify the viable neutrino mass spectra.

The result in chapter V was obtained by combining recent experimental data on neutrino masses and partial wave unitary bound. We got the lower bound on the lightest neutrino mass. It is greater than 6.11×10^{-4} eV for normal hierarchy. Moreover, we found that the inverted hierarchy case is incompatible with this model. For the result involving mixing parameters in chapter VI, we cannot constrain them in both hierarchies since the effect of mixing parameters do not rule out the perturbative region enough as their conservative range can be.

In summary, our results came from only $F^i \bar{F}^i \rightarrow A_L^{\ell,a} A_L^{\ell,a}$ and $F^i \bar{F}^j \rightarrow$

$A_L^{\ell,a} A_L^{\ell,b}$. It does not effective enough to claim on the bound of neutrino masses. To improve this theoretical bound, we could study more special symmetry model in the lepton sector to get more information about extra fermions or another gauge bosons (Alonso et al., 2016). Furthermore, there are some specific models which can also generate the neutrino mass known as seesaw-type I,II and III (Xing and Zhou, 2011) with different new physics particles. Lastly, we still look forward to an unexpected data in neutrino experiments for supporting the extension of standard model.





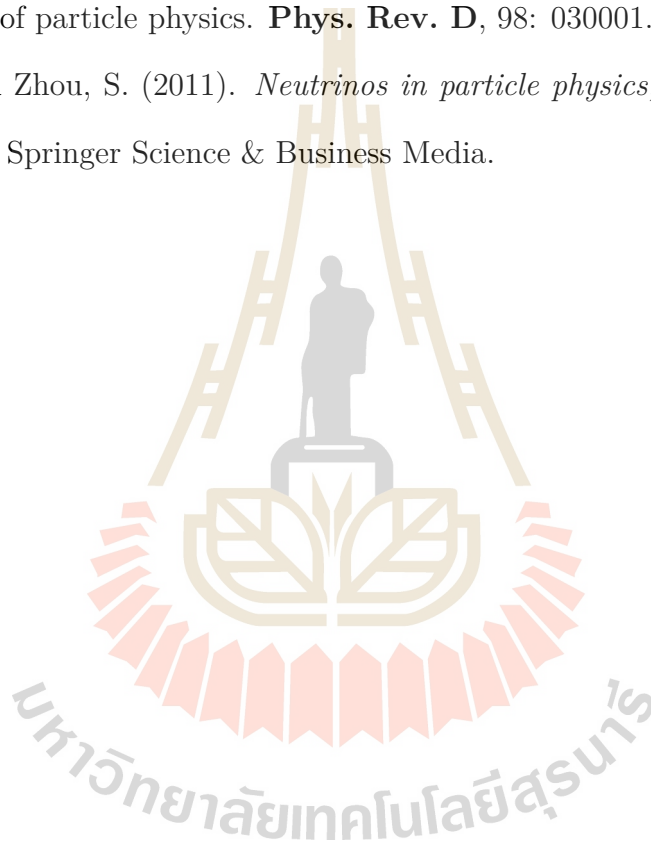
REFERENCES

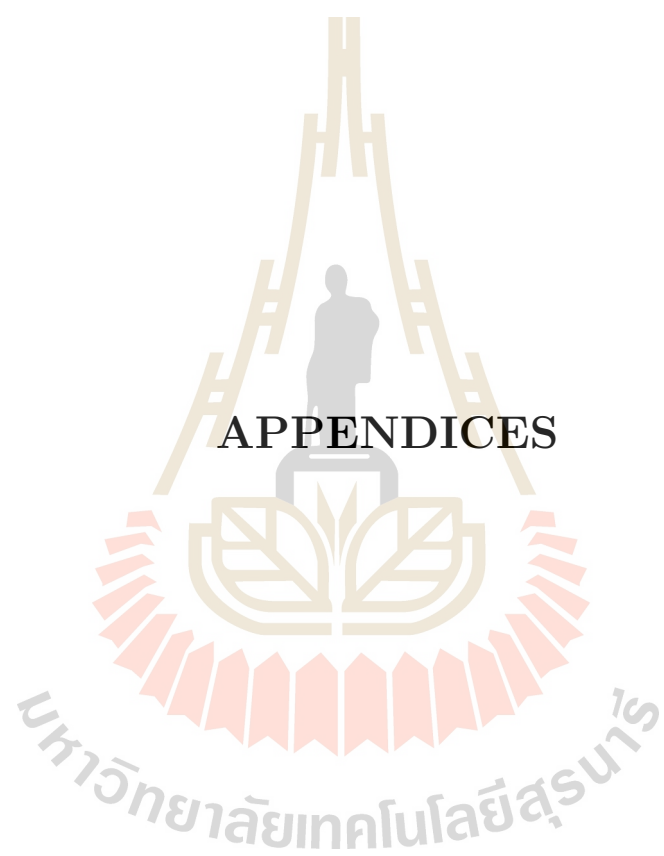
มหาวิทยาลัยเทคโนโลยีสุรนารี

REFERENCES

- Ahmad, Q. R., Allen, R. C., Andersen, T. C., Anglin, J., Buhler, G., Barton, J., Beier, E., Bercovitch, M., Bigu, J., Biller, S., Black, R., Blevis, I., Boardman, R., Boger, J., Bonvin, E., et al. (2001). Measurement of the rate of $\nu_e + d \rightarrow p + p + e^-$ interactions produced by 8B solar neutrinos at the Sudbury Neutrino Observatory. **Phys. Rev. Lett.** 87: 071301.
- Akhmedov, E. (2014). Majorana neutrinos and other majorana particles: Theory and experiment. **arXiv preprint arXiv:** 1412.3320.
- Alonso, R., Fernandez Martinez, E., Gavela, M., Grinstein, B., Merlo, L., and Quilez, P. (2016). Gauged lepton flavour. **Journal of High Energy Physics**, 2016(12): 119.
- Alonso, R., Gavela, M. B., Hernandez, D., and Merlo, L. (2012). On the Potential of Leptonic Minimal Flavour Violation. **Phys. Lett.**, B715: 194–198.
- Alonso, R., Gavela, M. B., Hernández, D., Merlo, L., and Rigolin, S. (2013a). Leptonic Dynamical Yukawa Couplings. **JHEP**, 08: 069.
- Alonso, R., Gavela, M. B., Isidori, G., and Maiani, L. (2013b). Neutrino Mixing and Masses from a Minimum Principle. **JHEP**, 11: 187.
- Fukuda, Y., Hayakawa, T., Ichihara, E., Inoue, K., Ishihara, K., Ishino, H., Itow, Y., Kajita, T., Kameda, J., Kasuga, S., Kobayashi, K., Kobayashi, Y., Kosho, Y., Miura, M., Nakahata, M., et al. (1998). Evidence for oscillation of atmospheric neutrinos. **Phys. Rev. Lett.** 81: 1562–1567.
- Lee, B. W., Quigg, C., and Thacker, H. B. (1977). Weak Interactions at Very High-Energies: The Role of the Higgs Boson Mass. **Phys. Rev.**, D16: 1519.

- Patrignani, C., Weinberg, D., Woody, C., Chivukula, R., Buchmueller, O., Kuyanov, Y. V., Blucher, E., Willocq, S., Höcker, A., Lippmann, C., et al. (2016). Review of particle physics. **Chin. Phys.**, 40: 100001.
- Schwartz, M. D. (2014). *Quantum Field Theory and the Standard Model*. Cambridge University Press.
- Tanabashi, M., Hagiwara, K., Hikasa, K., Nakamura, K., Sumino, et al. (2018). Review of particle physics. **Phys. Rev. D**, 98: 030001.
- Xing, Z. and Zhou, S. (2011). *Neutrinos in particle physics, astronomy and cosmology*. Springer Science & Business Media.





APPENDICES

APPENDIX A

STRUCTURE CONSTANTS

In flavor gauge symmetry $SU(3)_\ell$, There are eight generators. They are 3×3 matrices which called the Gell-mann matrices λ^a .

$$T^a \equiv \frac{1}{2} \lambda^a \quad (\text{A.1})$$

$$[T^a, T^b] = i f^{abc} T^c \quad (\text{A.2})$$

Since we have to diagonalize flavor mass matrix, Thus structure constants should be calculated Traditional $SU(3)$ generators can write in the term of new generators

$$T^3 = c_\alpha T^{3'} + s_\alpha T^{8'}, \quad (\text{A.3})$$

$$T^8 = -s_\alpha T^{3'} + c_\alpha T^{8'},$$

and the inverse relation is

$$T^{3'} = c_\alpha T^3 - s_\alpha T^8, \quad (\text{A.4})$$

$$T^{8'} = s_\alpha T^3 + c_\alpha T^8.$$

Then we use commutation relations $[T^a, T^b] = i f^{abc} T^c$ to determine new structure constants

For traditional structure constant $f^{123} = 1$, $f^{345} = -f^{367} = \frac{1}{2}$, $f^{458} =$

$f^{678} = \frac{\sqrt{3}}{2}$ and the commutations are

$$\begin{aligned} [T^1, T^2] &= if^{123}T^3 + if^{128}T^8 + if^{12c}T^c, \\ [T^4, T^5] &= if^{453}T^3 + if^{458}T^8 + if^{45c}T^c, \\ [T^6, T^7] &= if^{673}T^3 + if^{678}T^8 + if^{67c}T^c. \end{aligned} \tag{A.5}$$

Therefore, new structure constants are

$$\begin{aligned} f^{123} &= -f^{213} = c_\alpha \\ f^{128} &= -f^{218} = s_\alpha \\ f^{147} &= f^{516} = f^{246} = f^{257} = -f^{417} = -f^{156} = -f^{426} = -f^{527} = \frac{1}{2} \\ f^{345} &= -f^{435} = \frac{1}{2}c_\alpha - \frac{\sqrt{3}}{2}s_\alpha \\ f^{367} &= -f^{637} = -\frac{1}{2}c_\alpha - \frac{\sqrt{3}}{2}s_\alpha \\ f^{458} &= -f^{548} = \frac{\sqrt{3}}{2}c_\alpha + \frac{1}{2}s_\alpha \\ f^{678} &= -f^{768} = \frac{\sqrt{3}}{2}c_\alpha - \frac{1}{2}s_\alpha \end{aligned} \tag{A.6}$$

APPENDIX B

$$A_L^{\ell,a} A_L^{\ell,a} \rightarrow A_L^{\ell,b} A_L^{\ell,b}$$

Scalar products: $k_i(p_i)$ is an incoming(outgoing) gauge boson and $\epsilon_{k_i}(\epsilon_{p_i})$ is polarization of incoming(outgoing) gauge boson.

$$k_1 \cdot k_1 = k_2 \cdot k_2 = M_a^2$$

$$k_1 \cdot k_2 = \frac{s}{2} - M_a^2$$

$$p_1 \cdot p_1 = M_b^2$$

$$p_1 \cdot p_2 = \frac{s}{2} - M_b^2$$

$$k_1 \cdot p_1 = k_2 \cdot p_2 = -\frac{t}{2} + \frac{M_a^2 + M_b^2}{2}$$

$$k_1 \cdot p_2 = k_2 \cdot p_1 = -\frac{u}{2} + \frac{M_a^2 + M_b^2}{2}$$

$$\epsilon_{k_1} \cdot \epsilon_{k_1} = \epsilon_{k_2} \cdot \epsilon_{k_2} = \epsilon_{p_1} \cdot \epsilon_{p_1} = \epsilon_{p_2} \cdot \epsilon_{p_2} = -1$$

$$\epsilon_{k_1} \cdot \epsilon_{k_2} = \frac{s}{2M_a^2} - 1$$

$$\epsilon_{p_1} \cdot \epsilon_{p_2} = \frac{s}{2M_b^2} - 1$$

$$\epsilon_{k_1} \cdot \epsilon_{p_1} = \epsilon_{k_2} \cdot \epsilon_{p_2} = \frac{s}{4M_a M_b} \left(\sqrt{1 - \frac{4M_a^2}{s}} \sqrt{1 - \frac{4M_b^2}{s}} - x \right)$$

$$\epsilon_{k_1} \cdot \epsilon_{p_2} = \epsilon_{k_2} \cdot \epsilon_{p_1} = \frac{s}{4M_a M_b} \left(\sqrt{1 - \frac{4M_a^2}{s}} \sqrt{1 - \frac{4M_b^2}{s}} + x \right)$$

(B.1)

$$\epsilon_{k_1} \cdot k_1 = \epsilon_{k_2} \cdot k_2 = \epsilon_{p_1} \cdot p_1 = \epsilon_{p_2} \cdot p_1 = 0$$

$$\epsilon_{k_1} \cdot k_2 = \epsilon_{k_2} \cdot k_1 = \frac{s}{2M_a} \sqrt{1 - \frac{4M_a^2}{s}}$$

$$\epsilon_{p_1} \cdot p_2 = \epsilon_{p_2} \cdot p_1 = \frac{s}{2M_a} \sqrt{1 - \frac{4M_b^2}{s}}$$

$$\epsilon_{k_1} \cdot p_1 = \epsilon_{k_2} \cdot p_2 = \frac{s}{4M_a} \left(\sqrt{1 - \frac{4M_a^2}{s}} - \sqrt{1 - \frac{4M_b^2}{s}} x \right) \quad (\text{B.2})$$

$$\epsilon_{k_1} \cdot p_2 = \epsilon_{k_2} \cdot p_1 = \frac{s}{4M_a} \left(\sqrt{1 - \frac{4M_a^2}{s}} + \sqrt{1 - \frac{4M_b^2}{s}} x \right)$$

$$\epsilon_{p_1} \cdot k_1 = \epsilon_{p_2} \cdot k_2 = \frac{s}{4M_a} \left(\sqrt{1 - \frac{4M_b^2}{s}} - \sqrt{1 - \frac{4M_a^2}{s}} x \right)$$

$$\epsilon_{p_1} \cdot k_2 = \epsilon_{p_2} \cdot k_1 = \frac{s}{4M_a} \left(\sqrt{1 - \frac{4M_b^2}{s}} + \sqrt{1 - \frac{4M_a^2}{s}} x \right)$$

t-channel:

$$\begin{aligned}
\mathcal{M}_{A_L^{\ell,c}:t\text{-channel}} &= \epsilon_{k_1,\mu} \epsilon_{k_2,\nu} \epsilon_{p_1,\alpha}^* \epsilon_{p_2,\beta}^* \\
&\quad (-ig_A f^{abc})^2 \left(g^{\mu\alpha} (k_1 + p_1)^\lambda + g^{\alpha\lambda} (k_1 - 2p_1)^\mu + g^{\lambda\mu} (p_1 - 2k_1)^\alpha \right) \\
&\quad \frac{1}{t - M_c^2} \left(g^{\lambda\rho} - \frac{1}{M_c^2} (k_1 - p_1)^\lambda (p_2 - k_2)^\rho \right) \\
&\quad \left(g^{\nu\beta} (k_2 + p_2)^\rho + g^{\beta\rho} (k_2 - 2p_2)^\nu + g^{\rho\nu} (p_2 - 2k_2)^\beta \right) \\
\mathcal{M}_{A_L^{\ell,c}:t\text{-channel}} &= (-ig_A f^{abc})^2 \frac{1}{t - M_c^2} \\
&\quad \left(\epsilon_{k_1} \cdot \epsilon_{p_1}^* \left((k_1 + p_1) \cdot (k_2 + p_2) \epsilon_{k_2} \cdot \epsilon_{p_2}^* + \epsilon_{k_2} \cdot (k_2 - 2p_2) \epsilon_{p_2}^* \cdot (k_1 + p_1) \right. \right. \\
&\quad \left. \left. + \epsilon_{k_2} \cdot (k_1 + p_1) \epsilon_{p_2}^* \cdot (p_2 - 2k_2) \right) \right. \\
&\quad \left. + \epsilon_{k_1} \cdot (k_1 - 2p_1) \left(\epsilon_{p_1}^* \cdot (k_2 + p_2) \epsilon_{k_2} \cdot \epsilon_{p_2}^* + \epsilon_{p_1}^* \cdot \epsilon_{p_2}^* \epsilon_{k_2} \cdot (k_2 - 2p_2) \right) \right. \\
&\quad \left. + \epsilon_{p_1}^* \cdot \epsilon_{k_2} \epsilon_{p_2}^* \cdot (p_2 - 2k_2) \right) \\
&\quad \left. + \epsilon_{p_1}^* \cdot (p_1 - 2k_1) \left(\epsilon_{k_1} \cdot (k_2 + p_2) \epsilon_{k_2} \cdot \epsilon_{p_2}^* + \epsilon_{k_1} \cdot \epsilon_{p_2}^* \epsilon_{k_2} \cdot (k_2 - 2p_2) \right) \right. \\
&\quad \left. - \frac{1}{M_c^2} \left(\epsilon_{k_1} \cdot \epsilon_{p_1}^* (k_1 + p_1) (k_1 - p_1) + \epsilon_{p_1}^* \cdot (k_1 - p_1) \epsilon_{k_1} \cdot (k_1 - 2p_1) \right. \right. \\
&\quad \left. \left. + \epsilon_{p_1}^* \cdot (p_1 - 2k_1) \epsilon_{k_1} \cdot (k_1 - p_1) \right) \left((p_2 - k_2) \cdot (k_2 + p_2) \epsilon_{k_2} \cdot \epsilon_{p_2}^* \right. \right. \\
&\quad \left. \left. + \epsilon_{p_2}^* \cdot (p_2 - k_2) \epsilon_{k_2} \cdot (k_2 - 2p_2) + \epsilon_{k_2} \cdot \epsilon_{p_2}^* (p_2 - 2k_2) \right) \right)
\end{aligned} \tag{B.3}$$

u-channel:

$$\begin{aligned}
\mathcal{M}_{A_L^{\ell,c}:\text{u-channel}} &= \epsilon_{k_1,\mu} \epsilon_{k_2,\nu} \epsilon_{p_1,\alpha}^* \epsilon_{p_2,\beta}^* \\
&\quad (-ig_A f^{abc})^2 \left(g^{\mu\alpha} (k_1 + p_2)^\lambda + g^{\alpha\lambda} (k_1 - 2p_2)^\mu + g^{\lambda\mu} (p_2 - 2k_1)^\alpha \right) \\
&\quad \frac{1}{u - M_c^2} \left(g^{\lambda\rho} - \frac{1}{M_c^2} (k_1 - p_2)^\lambda (p_1 - k_2)^\rho \right) \\
&\quad \left(g^{\nu\beta} (k_2 + p_1)^\rho + g^{\beta\rho} (k_2 - 2p_1)^\nu + g^{\rho\nu} (p_1 - 2k_2)^\beta \right) \\
\mathcal{M}_{A_L^{\ell,c}:\text{u-channel}} &= (-ig_A f^{abc})^2 \frac{1}{u - M_c^2} \\
&\quad \left(\epsilon_{k_1} \cdot \epsilon_{p_1}^* \left((k_1 + p_2) \cdot (k_2 + p_1) \epsilon_{k_2} \cdot \epsilon_{p_2}^* + \epsilon_{k_2} \cdot (k_2 - 2p_2) \epsilon_{p_2}^* \cdot (k_1 + p_2) \right. \right. \\
&\quad \left. \left. + \epsilon_{k_2} \cdot (k_1 + p_2) \epsilon_{p_2}^* \cdot (p_1 - 2k_2) \right) \right. \\
&\quad \left. + \epsilon_{k_1} \cdot (k_1 - 2p_2) \left(\epsilon_{p_1}^* \cdot (k_2 + p_2) \epsilon_{k_2} \cdot \epsilon_{p_2}^* + \epsilon_{p_1}^* \cdot \epsilon_{p_2}^* \epsilon_{k_2} \cdot (k_2 - 2p_1) \right) \right. \\
&\quad \left. + \epsilon_{p_1}^* \cdot \epsilon_{k_2} \epsilon_{p_2}^* \cdot (p_1 - 2k_2) \right) \\
&\quad \left. + \epsilon_{p_1}^* \cdot (p_2 - 2k_1) \left(\epsilon_{k_1} \cdot (k_2 + p_1) \epsilon_{k_2} \cdot \epsilon_{p_2}^* + \epsilon_{k_1} \cdot \epsilon_{p_2}^* \epsilon_{k_2} \cdot (k_2 - 2p_2) \right) \right. \\
&\quad \left. - \frac{1}{M_c^2} \left(\epsilon_{k_1} \cdot \epsilon_{p_1}^* (k_1 + p_2) (k_1 - p_2) + \epsilon_{p_1}^* \cdot (k_1 - p_1) \epsilon_{k_1} \cdot (k_1 - 2p_2) \right. \right. \\
&\quad \left. \left. + \epsilon_{p_1}^* \cdot (p_2 - 2k_1) \epsilon_{k_1} \cdot (k_1 - p_2) \right) \left((p_1 - k_2) \cdot (k_2 + p_1) \epsilon_{k_2} \cdot \epsilon_{p_2}^* \right. \right. \\
&\quad \left. \left. + \epsilon_{p_2}^* \cdot (p_1 - k_2) \epsilon_{k_2} \cdot (k_2 - 2p_1) + \epsilon_{k_2} \cdot \epsilon_{p_2}^* (p_1 - 2k_2) \right) \right)
\end{aligned} \tag{B.4}$$

APPENDIX C

$$A_L^{\ell,a} A_L^{\ell,b} \rightarrow A_L^{\ell,a} A_L^{\ell,b}$$

Scalar products: $k_i(p_i)$ is an incoming(outgoing) gauge boson and $\epsilon_{k_i}(\epsilon_{p_i})$ is polarization of incoming(outgoing) gauge boson.

$$\begin{aligned}
 k_1 \cdot k_1 &= M_a^2, & k_2 \cdot k_2 &= M_b^2, \\
 k_1 \cdot k_2 &= \sqrt{M_a^2 + p_i^2} \sqrt{M_b^2 + p_i^2 + p_i^2}, \\
 p_1 \cdot p_2 &= \sqrt{M_a^2 + p_f^2} \sqrt{M_b^2 + p_f^2 + p_f^2}, \\
 k_{1(2)} \cdot p_{1(2)} &= \sqrt{M_{a(b)}^2 + p_f^2} \sqrt{M_{a(b)}^2 + p_i^2} - p_i p_f x \\
 k_{1(2)} \cdot p_{2(1)} &= \sqrt{M_a^2 + p_{i(f)}^2} \sqrt{M_b^2 + p_{f(i)}^2} + p_i p_f x \\
 \epsilon_{k_1} \cdot \epsilon_{k_1} &= \epsilon_{k_2} \cdot \epsilon_{k_2} = \epsilon_{p_1} \cdot \epsilon_{p_1} = \epsilon_{p_2} \cdot \epsilon_{p_2} = -1, \\
 \epsilon_{k_1} \cdot \epsilon_{k_2} &= \frac{\sqrt{M_a^2 + p_i^2} \sqrt{M_b^2 + p_i^2 + p_i^2}}{M_a M_b} \\
 \epsilon_{p_1} \cdot \epsilon_{p_2} &= \frac{\sqrt{M_a^2 + p_f^2} \sqrt{M_b^2 + p_f^2 + p_f^2}}{M_a M_b}, \\
 \epsilon_{k_{1(2)}} \cdot \epsilon_{p_{1(2)}} &= \frac{p_f p_i - x \sqrt{M_{a(b)}^2 + p_f^2} \sqrt{M_{a(b)}^2 + p_i^2}}{M_a^2} \\
 \epsilon_{k_{1(2)}} \cdot \epsilon_{p_{2(1)}} &= \frac{p_f p_i + x \sqrt{M_a^2 + p_{i(f)}^2} \sqrt{M_b^2 + p_{f(i)}^2}}{M_a M_b},
 \end{aligned} \tag{C.1}$$

$$\epsilon_{k_1} \cdot k_1 = \epsilon_{k_2} \cdot k_2 = \epsilon_{p_1} \cdot p_1 = \epsilon_{p_2} \cdot p_1 = 0$$

$$\epsilon_{k_1} \cdot k_2 = \frac{p_i}{M_a} (\sqrt{M_a^2 + p_i^2} + \sqrt{M_b^2 + p_i^2})$$

$$\epsilon_{k_2} \cdot k_1 = \frac{p_i}{M_b} (\sqrt{M_a^2 + p_i^2} + \sqrt{M_b^2 + p_i^2})$$

$$\epsilon_{p_1} \cdot p_2 = \frac{p_i}{M_b} (\sqrt{M_a^2 + p_i^2} + \sqrt{M_b^2 + p_i^2})$$

$$\epsilon_{p_2} \cdot p_1 = \frac{p_f}{M_b} (\sqrt{M_a^2 + p_f^2} + \sqrt{M_b^2 + p_f^2})$$

$$\epsilon_{k_1} \cdot p_1 = \frac{p_i \sqrt{M_a^2 + p_i^2} - p_f x \sqrt{M_a^2 + p_i^2}}{M_a}$$

$$\epsilon_{k_2} \cdot p_2 = \frac{p_i \sqrt{M_b^2 + p_f^2} - p_f x \sqrt{M_b^2 + p_i^2}}{M_b}$$

$$\epsilon_{k_1} \cdot p_2 = \frac{p_f x \sqrt{M_a^2 + p_i^2} + p_i \sqrt{M_b^2 + p_i^2}}{M_a}$$

$$\epsilon_{k_2} \cdot p_1 = \frac{p_i}{M_b} (\sqrt{M_a^2 + p_i^2} + \sqrt{M_b^2 + p_i^2})$$

$$\epsilon_{p_1} \cdot k_1 = \frac{p_f \sqrt{M_a^2 + p_i^2} - p_i x \sqrt{M_b^2 + p_f^2}}{M_a}$$

$$\epsilon_{p_2} \cdot k_2 = \frac{p_f \sqrt{M_a^2 + p_i^2} - p_i x \sqrt{M_b^2 + p_f^2}}{M_b}$$

$$\epsilon_{p_1} \cdot k_2 = \frac{p_i x \sqrt{M_a^2 + p_f^2} + p_f \sqrt{M_b^2 + p_i^2}}{M_a}$$

$$\epsilon_{p_2} \cdot k_1 = \frac{p_f \sqrt{M_a^2 + p_i^2} + p_i x \sqrt{M_b^2 + p_f^2}}{M_b}$$

(C.2)

s-channel:

$$\begin{aligned}
\mathcal{M}_{A_L^{\ell,c}:\text{s-channel}} &= \epsilon_{k_1,\mu} \epsilon_{k_2,\nu} \epsilon_{p_1,\alpha}^* \epsilon_{p_2,\beta}^* \\
&\quad \left(-ig_A f^{abc} \right)^2 \left(g^{\mu\lambda} (2k_1 + k_2)^\nu + g^{\lambda\nu} (-k_1 - 2k_2)^\mu + g^{\nu\mu} (-k_1 + k_2)^\lambda \right) \\
&\quad \frac{1}{s - M_c^2} \left(g^{\lambda\rho} - \frac{1}{M_c^2} (k_1 + k_2)^\lambda (p_1 + p_2)^\rho \right) \\
&\quad \left(g^{\alpha\beta} (p_2 - p_1)^\rho + g^{\beta\rho} (-p_1 - 2p_2)^\alpha + g^{\rho\alpha} (2p_1 + p_2)^\beta \right) \\
\mathcal{M}_{A_L^{\ell,c}:\text{s-channel}} &= (-ig_A f^{abc})^2 \frac{1}{s - M_c^2} \\
&\quad \left(\epsilon_{k_2} \cdot (2k_1 + k_2) \left(\epsilon_{k_1} \cdot (p_2 - p_1) \epsilon_{p_1}^* \cdot \epsilon_{p_2}^* + \epsilon_{k_1} \cdot \epsilon_{p_2}^* \epsilon_{p_1} \cdot (-p_1 - 2p_2) \right. \right. \\
&\quad \left. \left. + \epsilon_{k_1} \cdot \epsilon_{p_1}^* \epsilon_{p_2}^* \cdot (2p_1 + p_2) \right) + \epsilon_{k_1} \cdot (-k_1 - 2k_2) \left(\epsilon_{k_2} \cdot (p_2 - p_1) \epsilon_{p_1}^* \cdot \epsilon_{p_2}^* \right. \right. \\
&\quad \left. \left. + \epsilon_{k_2} \cdot \epsilon_{p_2}^* \epsilon_{p_1}^* \cdot (-p_1 - 2p_2) + \epsilon_{k_2} \cdot \epsilon_{p_1}^* \epsilon_{p_2}^* \cdot (2p_1 + p_2) \right) \right. \\
&\quad \left. + \epsilon_{k_1} \cdot \epsilon_{k_2} \left((-k_1 + k_2) \cdot (p_2 - p_1) \epsilon_{p_1}^* \cdot \epsilon_{p_2}^* \right. \right. \\
&\quad \left. \left. + (-k_1 + k_2) \cdot \epsilon_{p_2}^* \epsilon_{p_1}^* \cdot (-p_1 - 2p_2) + (-k_1 + k_2) \cdot \epsilon_{p_1}^* \epsilon_{p_2}^* \cdot (2p_1 + p_2) \right) \right. \\
&\quad \left. - \frac{1}{M_c^2} \left(\epsilon_{k_2} \cdot (2k_1 + k_2) \epsilon_{k_1} \cdot (k_1 + k_2) + \epsilon_{k_2} \cdot (k_1 + k_2) \epsilon_{k_1} \cdot (-k_1 - 2k_2) \right. \right. \\
&\quad \left. \left. + \epsilon_{k_1} \cdot \epsilon_{k_2} (-k_1 + k_2) \cdot (k_1 + k_2) \right) \left(\epsilon_{p_1}^* \cdot \epsilon_{p_2}^* (p_1 + p_2) \cdot (p_2 - p_1) \right. \right. \\
&\quad \left. \left. + \epsilon_{p_1}^* \cdot (-p_1 - 2p_2) (p_1 + p_2) \cdot \epsilon_{p_2}^* + \epsilon_{p_1}^* \cdot (p_1 + p_2) \epsilon_{p_2}^* \cdot (2p_1 + p_2) \right) \right) \\
\end{aligned} \tag{C.3}$$

CURRICULUM VITAE

Name: Wararat Treesukrat

Date of Birth: January 12, 1994

Place of Birth: Phrae, Thailand

Education:

2016, B. Sc. Department of Physics, Srinakharinwirot University Thailand.

Publications:

W Sreethawong, W Treesukrat and P Uttayarat, Neutrino spectrum in $SU(3)_\ell \times SU(3)_E$ gauged lepton flavor model, Journal of Physics: Conference Series, Volume 1144, conference 1.

